Fuel Processing Technology 265 (2024) 108149

Contents lists available at ScienceDirect

Fuel Processing Technology

journal homepage: www.elsevier.com/locate/fuproc

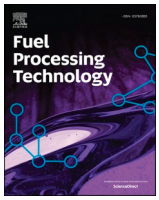

Impact of press channel diameter-to-length ratio on the mechanical properties of biomass pellets during storage

Abdullah Sadeq *, Swantje Pietsch-Braune, Stefan Heinrich

Institute of Solids Process Engineering and Particle Technology, Hamburg University of Technology, 21073 Hamburg, Germany

ARTICLE INFO

Keywords:
Biomass pellet
Pelleting process
Storage
Microcomputed tomography
Porosity distribution
Mechanical stability

ABSTRACT

This study investigates the effects of press channel length on the quality of wood pellets, focusing on key aspects such as density, radial porosity distribution, and mechanical stability, both at the time of delivery and during storage. Wood pellets were produced using press channels with diameter-to-length (D/L) ratios of 1:3, 1:4, and 1:5 to evaluate how variations in die geometry influence pellet quality. Micro-computed tomography (μCT) analysis indicates that the D/L ratio of the press channel significantly impacts the porosity within the pellets. Short press channels are associated with great variability in the radial porosity distribution of the wood pellets, while longer press channels lead to uniformly low porosity over the radius. Furthermore, pellets produced with longer press channels exhibit a smoother surface with fewer cracks and greater resistance to structural degradation under varying humidity conditions. Although high-density pellets show improved mechanical strength and recovery potential in humid environments, remaining damage in the form of cracks and alterations in radial porosity distribution lead to reduced strength compared to their initial state.

1. Introduction

Wood pellets are a climate-friendly alternative to fossil fuels, providing a high energy density and emitting lower levels of carbon dioxide [1]. They offer advantages such as easier handling and lower risks of dust explosion compared to loose wood shavings [2–5].

To ensure resistance to the mechanical loads encountered during transportation, wood pellets must exhibit high mechanical durability. Pellets with low mechanical durability tend to break more easily, resulting in a higher proportion of fines within the bulk. This negatively impacts their energy density, flow properties, and storage capacity [6–8]. The durability of wood pellets is typically determined using a pellet tumbler test, which simulates the mechanical loads during pellet conveying. According to the DIN EN ISO 17225-2 standard [9], wood pellets must achieve a durability of 97.5 % to be certified as *EN Plus A1*, i.e. they are of the highest quality. Even high-quality pellets can experience structural and stability changes during extended storage with fluctuating humidity. Therefore, in this paper correlations between pelleting conditions, mechanical properties of wood pellets and their storage stability are established.

1.1. Pelleting process

Previous studies have identified several parameters during the pelleting process that affect the quality of wood pellets. Water content and die temperature during the densification step have a greater impact on pellet density and durability than wood shaving size [6,8,10–14]. However, an optimal size distribution can also contribute to pellet stability, whereby the mechanical properties of raw materials and their particle size distribution play an interrelated role [15,16]. Therefore, different size distributions are found to be suitable for pelleting of different biomass sources [4,6,17–19]. A study on wood pellets made from four different size fractions of pine wood shavings with a maximum shaving size of 8 mm showed similar energy consumption and similar pellet density, though pellets from smaller size fractions had a higher compressive strength [20]. However, some studies report a high pellet density and pellet stability by setting smaller size ranges. It is assumed to enable an increased contact area between the particles and improved binding properties [6,17–19].

Lignin is one of the binding components responsible for maintaining the final pellet structure and thus final pellet stability [10,21–24]. The concentration depends on the biomass type used for the pellets. Increased water content or high die temperature transitions lignin from

* Corresponding author at: Denickestrasse 15, 21073 Hamburg, Germany.
E-mail address: abdullah.sadeq@tuhh.de (A. Sadeq).

https://doi.org/10.1016/j.fuproc.2024.108149
Received 5 September 2024; Received in revised form 15 October 2024; Accepted 22 October 2024
Available online 30 October 2024

a glassy to a rubbery state, enhancing the flowability of the wood shavings during pelleting [12,24–26] and leading to reduced energy consumption and high pellet density. Carone et al. [7] observed that a high process temperature of about 150 °C, a water content of 10 wt.-% and reduced particle sizes of olive tree pruning residues allow obtaining pellets with high density during single pelleting tests. The pelleting pressure was set at 170–180 MPa. The predominant role of temperature was evident as high density pellets were also obtained with a reduced pelleting pressure of 70 MPa, while the temperature was maintained at 150 °C. Also other studies [27–29] attribute a greater influence of the temperature than of the pelleting pressure on the final stability of biomass pellets.

An investigation of wheat and barley straw, corn stover and switchgrass pellets revealed that a water content of 12 wt.-% and a reduced hammer mill screen size of 0.8 mm for the raw materials increased the density of pellets [17]. Stelte et al. [21] found for beech, spruce and straw pellets that the best stability was achieved at a water content in the range between 10 and 15 wt.-% and that a water content of more than 20 wt.-% did not result in stable pellets. The authors explained this by the possibility that many hydrogen bonds between the wood polymers are replaced by bonds to water molecules, which reduces the strength of the pellet.

In summary, the lubrication effect due to high die temperature and suitable water content as well as a higher adhesion between smaller particle have been shown to be crucial for high density and durability pellets.

These factors and the design of the die determine the required backpressure in the press channel for continuous pelleting. The backpressure is caused in particular by the accumulation of biomass in the press channel and thus by the friction between the wood shavings and the die wall leading to higher die temperature [2,6,15,21,30,31]. The longer the press channel, i.e. the smaller the ratio of diameter-to-length (D/L) of the press channel, the exponentially higher the back pressure that must be overcome [15,16]. In another study [32], cattle feed pellets were produced with dies of different D/L ratios (D/L 1:3, 1:6, and 1:8) and compared for their stability with a pellet hardness tester. The press channel with the lowest D/L ratio led to a high specific energy consumption and pellets of high density and hardness.

Pellets that are produced in large-scale flat or ring die presses, where wood shavings are pressed through an open die with conical inlet channels, exhibit conically shaped layers. They have higher mechanical strength compared to pellets from closed die single pelleting tests, which have transverse layers [33]. Hu et al. [34] studied specific energy consumption during rice straw pelleting using an open die setup, focusing on countersink angle β, compaction rate, moisture content, and the D/L ratio of the press channel. They found the lowest energy consumption at $\beta = 60.5°$, with minimal impact from β compared to other parameters. Nielsen et al. [30] emphasized that inlet depth (h) and inactive areas in the press channel must be considered to compare results with large-scale pelleting plants. Deeper inlets were associated with higher pelleting force and energy consumption [35]. Additionally, Nielsen et al. [36] introduced the AR design parameter, relating active, transition, and inactive areas in the press channel, influencing the steepness of pellet layer profiles. Layer shape variation was observed, likely due to the non-continuum behavior of feedstock particles of different sizes.

Using a 3D reconstruction of commercial spruce and mixed pellets from μCT measurements, Sadeq et al. [37] confirmed that the gaps between wood shavings in a pellet follow the layer shape. By distinguishing between total porosity, which takes all pores into account, and gap porosity, which is the ratio between the volume of the gaps and the volume of the pellet, the predominant influence of gap porosity on the stability of the pellet was shown [38]. The higher the gap porosity, the lower the mechanical strength of the pellets. In the study of Tenorio et al. [39], variations of the density were shown at the internal level of pellets made from empty fruit bunches and oil palm fruit mesocarp. Density variations in radial direction within pellets might occur due to the radial stress distribution in the press channel, caused by the occurring frictional forces and variations of temperature [14,31].

After biomass shavings have been pressed, it is often observed that the resulting pellets begin to expand in the opposite direction to the previous loading direction until a constant volume is reached. This is known as the spring-back effect and, as a result, the relaxed density of the pellets is significantly lower than immediately after pressing [10,17,24,40–45]. This is attributed to the rheological behavior of the polymer components. The elasticity of polymers such as cellulose, hemicellulose and lignin causes them to return to their original, undeformed structure after compression. If the bond between the particles is weak, the pellets expand, resulting in a decrease in density [46]. Therefore, an optimum setting of parameters such as a temperature above the glass transition temperature of the binding components, a moderate water content, small particle size ranges and high pressing pressure can help to limit the springback effect. In the case of closed die single pelleting tests, holding the punch at high pressure for 60 s can also lead to a reduction in the spring-back effect [17,40,41,47]. As this is not possible in open-die setups, the pellets are usually cooled after emerging from the die. The binding components can quickly transition from their rubbery state back to their glassy state and the pellet structure is retained [2,48,49]. In summary, previous studies investigated the influence of process and material conditions with regard to pellet apparent density and stability. However, to the best of the authors' knowledge, a variation of the radial pellet density or porosity obtained by different D/L ratios of the press channel and its effect on pellet stability has not yet been investigated.

1.2. Storage effects

During long-term storage or overseas transport, wood pellets are exposed to fluctuating humidity levels, leading to changes in their water content. The sorption of water vapor follows the type II isotherms according to the van der Waals classification. After the subsequent desorption of water vapor, a hysteresis is formed, which is assumed to be a result of the "ink bottle effect" [37,50–54]. Studies have shown that increased humidity leads to swelling of wood pellets and an increased surface roughness due to a rising number of surface cracks [37,55–57]. While Hartley and Wood [58] described the relationship between volumetric swelling and water content with a power law function, others [59,60] described it with a polynomial of degree 5 or [37] for spruce and mixed pellets with an initially linear curve and a subsequent exponential increase when higher water contents are achieved above the saturation vapor pressure. This shows how strongly wood pellets of different origins differ from each other in terms of their interaction with water. The swelling of wood pellets can be attributed to the swelling of the individual wood shavings, which occurs as their cell walls absorb water and consequently increase in volume [37,61,62]. The extent to which pellet swelling occurs seems to depend on the type of exposure and the corresponding water adsorption rate. Setting a relative humidity of over 95 % in a humidity chamber to increase the water content in a shorter time leads to greater swelling than exposing wood pellets to salt solutions in a desiccator. Here, the water content increases gently over a longer period of time, during which the pellet matrix can relax during volumetric expansion [37,59,60,63].

Deng et al. [55] showed that changes in single pellet density are associated with a corresponding change in the density and durability of the pellet bulk.

High humidity can significantly reduce the stability of wood pellets by softening lignin, with effects intensified at temperatures around 30 °C [10,24–26,38,64]. Compression and bending tests show that pellets with water content above 10 wt.-% experience decreased strength [38,56,64–66]. Axial and diametrical compression tests reveal that after exceeding the proportional stress limit, continuous loading leads to plastic deformation and failure, though yield points are less clear in diametrical tests due to ongoing densification [38].

Wet wood pellets can partially recover their stability upon re-drying, but often retain increased porosity and gaps between shavings [37,38]. Long-term storage with constantly fluctuating water content increases porosity and decreases stability, particularly when the saturation vapor pressure is exceeded.

Controlling environmental conditions such as temperature and humidity during storage is both difficult and ecologically unreasonable. As a result, the critical water content of 10 wt.-% specified in DIN EN ISO 17225-2 can be exceeded multiple times, leading to significant variations in the mechanical properties of wood pellets from their initial state. It is necessary to investigate whether optimizing conditions during the pelleting process can positively influence the storage stability of wood pellets. Therefore, in this study, wood shavings of the same origin with similar water content and size distribution were prepared and densified with a flat die press using different die geometries with a D/L ratio of 1:3 (diameter 6 mm, length 18 mm), 1:4 (diameter 6 mm, length 24 mm) and 1:5 (diameter 6 mm, length 30 mm). Subsequently, the obtained pellets of different densities were analyzed for their mechanical properties in their initial state and during storage with cyclic humidity changes.

2. Materials and methods

2.1. Preparation of the wood shavings

The spruce wood shavings were provided by the company Pfeifer Holz GmbH (Uelzen, Germany). Following a drying process in a belt dryer, the wood shavings exhibited a water content of 4.5 wt.-%. The wood shavings had maximum dimensions of 30 mm in length and 8 mm in width, and a bulk density of 140 kg/m^3. The **bulk density ρ_{Bulk}** was derived from the ratio of specimen to the volume it occupies in a cylindrical vessel.

The wood shavings were further processed in cooperation with the Amandus Kahl GmbH & Co. KG (Reinbek, Germany). Initially, their size were reduced using a roller mill of type 33–390 equipped with two rollers, operating at 166 rpm with a roller speed set at 2.28 m/s. After milling, the wood shavings attained an x_{50} size of 1218 μm. As their water content was low at a process temperature of 71 °C, the milled wood shavings were moistened and soaked for 12 h. Before pelleting, the wood shavings were mixed with water in an MIT turbomixer for 30 s to achieve the desired water content of approximately 9 wt.-%.

To determine the **particle size distribution** of the raw wood shavings, sieving was performed for 5 min at 60 % of the maximum amplitude using the Retsch AS200 Control (Retsch Technology, Germany). For this purpose, sieves with mesh sizes of: 5.6, 4, 2.8, 2.0, 1.6, 1.0, 0.45 and 0.25 mm were selected. Furthermore, the size distribution was assessed optically using the Camsizer XT (Retsch Technology, Germany) by analyzing the $x_{c,min}$, as it correlates with the relevant width for sieving. The **median particle size x_{50}** was obtained by linear interpolation from the particle size distributions. To compare the size of raw wood shavings with the size of wood shavings in wood pellets, 300 g of wood pellets were disintegrated in 2 l of distilled water at a temperature of 80 °C and then dried in an oven at 60 °C until a water content of about 7 wt.-% was reached. The size of these wood shavings were analyzed analogously.

The **water content (wc)** of both wood shavings and pellets was determined as the percentage of the mass of evaporated water (m_{water}) to the total mass ($m_{water} + m_{dry}$) after subjecting at least 2 g of moist material to drying at 105 °C in a drying oven for 12 h.

$$wc\ [wt.-\%] = \frac{m_{water}}{m_{dry} + m_{water}} \bullet 100\% \quad (1)$$

The measurement of the water content was performed in triplicate.

2.2. Pelleting process

The pelleting process was carried out with two rotating steel rollers in a flat die press of type 14–175 from Amandus Kahl GmbH & Co. KG (Germany). With a pressure of up to 13 bar, this press can continuously produce up to 50 kg/h of pellets. At 112 rpm, a roller speed of 0.73 m/s was set to densify the manually fed wood shavings into pellets. To cut the pellets emerging from the die, the distance between the cutting blade and the exit of the die was adjusted to 37 mm.

In order to obtain pellets of different densities, dies that have press channels with a diameter of 6 mm and differ in their length were chosen resulting in different diameter (D) to length (L) ratios as illustrated in Fig. 1. For example, for a D/L ratio of 1:3 (diameter of 6 mm, length of 18 mm), the die type 122,997 was used. For a ratio of 1:4 (diameter of 6 mm, length of 24 mm) and 1:5 (diameter of 6 mm, length of 30 mm), die types 12,299 and 121,543 respectively were chosen. All press channels of the dies are cylindrical with an identical conical shaped inlet. The conical inlets have a countersink angle of 30° with a depth of 3.7 mm. The wood pellets produced accordingly are referred to in this study as 1:3, 1:4 and 1:5 wood pellets.

The **die temperature [°C]** was measured with a thermocouple located in the outer part of the flat die. During the pelleting process, the average power of the electrical current consumed by the pellet press was determined. From the difference between the average power during pelleting and the idle power, the net power was calculated. The **specific energy consumption [kWh/kg]** was calculated as the product of the net power and the process time, normalized by the total mass of wood

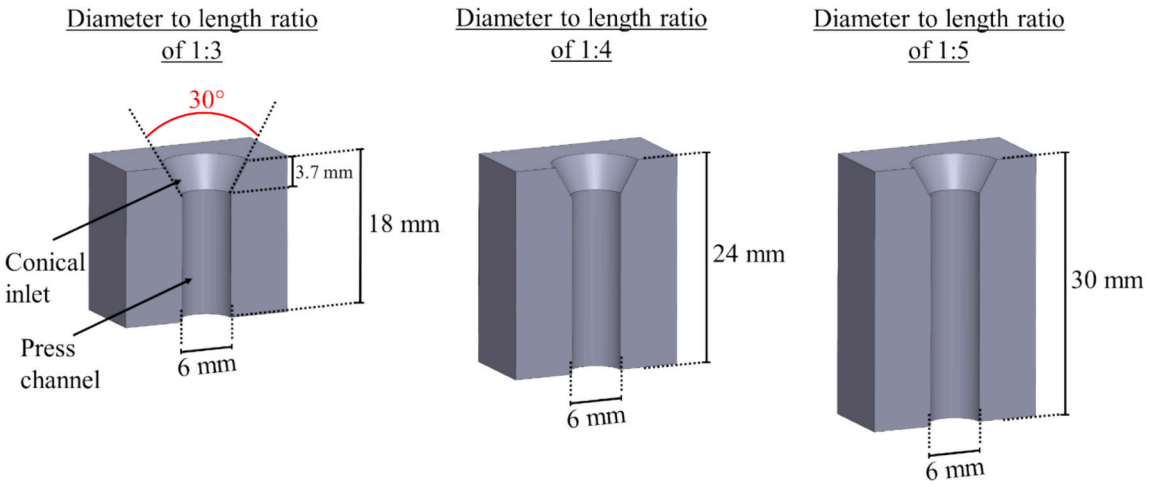

Fig. 1. Cross section of press channels of different dimensions used for pelleting 1:3, 1:4 and 1:5 wood pellets.

shavings used. The **throughput [kg/h]** was obtained from the mass of wood pellets exiting the flat die press over time. After pelleting, the pellets were cooled to ambient temperature.

2.3. Dynamic vapor sorption

Sorption isotherms were determined with the Dynamic Vapor Sorption (DVS) Resolution apparatus (Surface Measurement Systems Ltd., United Kingdom). Wood pellet fractions of about 80 mg were used for measurement. After an initial drying stage at 20 °C at 0 % relative humidity (rh), the rh was increased stepwise by 10 %, when an equilibrium (dm/dt $\leq$ 0.001 %/min) was reached. Once the sorption had been determined at a max. rh of 90 %, a 10 % stepwise decrease of the rh was performed to investigate desorption behavior. The equilibrium water content was calculated from the obtained mass at each level of rh using the eq. (1).

2.4. Conditioning

To enable a good comparison with the findings from literature, pellets were conditioned in a similar way as described in [37,38]. Prior to investigation of the mechanical properties of single pellets, their irregular shaped cut ends were sanded using the Disc Sander BTS700 (Scheppach, Germany) with a sandpaper of a grit size of 80 µm. A standardized pellet length of 18 $\pm$ 2 mm was set to reduce the scatter in the results of the mechanical tests. During preparation of the wood pellets, it was observed that compared to 1:4 and 1:5, the 1:3 wood pellets were difficult to handle due to their tendency to break easily.

Besides the pellet shape, different water contents were adjusted. To reach a water content of approximately 0.5 wt.-%, wood pellets were subjected to drying in an oven at 105 °C for 24 h. Water contents ranging between 4 and 12 wt.-% were attained by exposing the pellets to the desired humidity for seven days in the climate chamber ICH110 (Memmert GmbH & Co. KG, Germany). Values exceeding 12 wt.-% were obtained by using a self-made climate chamber with an ultrasonic humidifier and fans providing a uniform distribution of the humid air. In this setup, pellets were conditioned above the saturation vapor pressure at 20 °C. Throughout the process, temperature and humidity were monitored using two DKRF400 sensors placed in the lower and upper part of the climate chamber. After conditioning, the pellets were sealed in separate reaction tubes for seven days to ensure uniform water distribution within each pellet and to prevent subsequent alterations. Measurement of the water content at each state was performed as described in section 2.1.

2.5. Structural properties

The **pellet's apparent density ρ_{app}** was determined by dividing the mass by its cylindrical volume (V_{Pellet}). The volume of the cylindrical pellet was calculated using the known dimensions (length and diameter) measured with an outside micrometer according do DIN 863–1 [67]:

$$V_{Pellet} = l \cdot \frac{\pi}{4} d^2 \tag{2}$$

The **true density ρ_{true}** was obtained by using the helium pycnometer AccuPyc 1130 (Micromeritics Instrument Corporation, USA).

The **total porosity ε_{total}** was calculated by dividing the total void volume (V_{tv}) by the volume of the pellet (V_{Pellet}), using the following equation:

$$\varepsilon_{total}\,[-] = \frac{V_{tv}}{V_{Pellet}}, \tag{3}$$

whereby the total void volume of a pellet was determined from subtracting the volume of the pellet from the theoretical volume occupied by the wood shavings (V_{solids}). V_{solids} was derived from the ratio of the pellet mass in its initial dry state and its true density.

In order to characterize wood pellets during storage, the swelling behavior, changes in density and porosity as well as the degree of saturation were investigated. 210 wood pellets, consisting of 70 of each pellet type, were used for this part of the study. The 70 pellets of each type were divided into seven batches of ten wood pellets. After an initial drying process in the oven, they were humidified to attain a defined water content. Different water contents ranging between 0.5 and 15 wt.-% were set for each batch. Following this, they underwent a re-drying process as described in section 2.4. After each conditioning step, individual wood pellets were evaluated for their diameter and length in accordance with DIN 863–1 [67], and its mass was measured with an analytic balance.

Volumetric changes, e.g. **volumetric swelling,** was then determined from the ratio of the volume of a conditioned pellet to the volume of its initial dry state. To assess **changes in radial in longitudinal** direction, the pellet diameter and length were used, respectively. The same procedure was employed for **changes in apparent density** and **total porosity**.

The **degree of saturation** (S) was calculated by dividing the volume of water-filled voids by the total void volume (V_{tv}).

$$S = \frac{V_{wfv}}{V_{Pellet} - V_{solid}} = \frac{V_{wfv}}{V_{tv}} \tag{4}$$

The volume of water-filled voids (V_{wfv}) can be approximated theoretically by dividing the calculated water mass within the wood pellet, derived from its water content, from the density of water (998 kg/m^3). A degree of saturation value of 1 signifies that the total void volume is entirely filled with water, whereas a value of 0 indicates that the total void volume contains no water.

2.6. Image processing

For determination of the internal pellet structure, **x-Ray microcomputed tomography** (µCT) was performed using the µCT 35 from SCANCO Medical AG (Switzerland). The measurement was run at 177 mA and 45 keV and the spatial resolution of the acquired images was 6 µm. Wood pellets were inserted into separate x-ray-tubes and sealed to prevent interactions with the ambient air. The measurements were conducted with wood pellets in their initial dry, wet and re-dried states.

To process the image data, Avizo software (Thermofisher Scientific, version 2022.1) was used. With that software the gap porosity, i.e. the ratio between the volume of the detected voids and the volume of the pellet, could be determined by the following procedure:

In a pre-processing step, unused areas of the image were cropped to reduce the data size. The orientation of the image was then rotated to align the longitudinal direction of the pellet with the z-axis. In this way, the geometry-dependent properties of wood pellets can be analyzed in the subsequent steps.

To reduce the apparent noise and improve the contrast of the image, non-local mean filtering was performed (*Filtered*, Fig. 2). The two material phases, wood and air, could be identified as two distributions in the resulting histogram. The peak with a gray value of approximately 155 represents the wood phase due to the higher density and thus higher attenuation, the peak with a gray value of approximately 65 represents the air. Despite non-local mean filtering, the two distributions partially overlap, which is due to the image noise and the partial volume effect. To separate the specimen from the background, a threshold was set at 120 to allow a pre-assumption of the wood phase. All gray values below the threshold were assigned the value zero (air) and all gray values above the threshold were assigned the value one (wood), resulting in a binary image (*Binarized*, Fig. 2). It should be noted that with this threshold approach, some gray values can be assigned to the wrong material phase to a certain extent due to the superposition. A systematic error is therefore correspondingly present. In the next step, a morphological image processing procedure described by [68] was used. This is

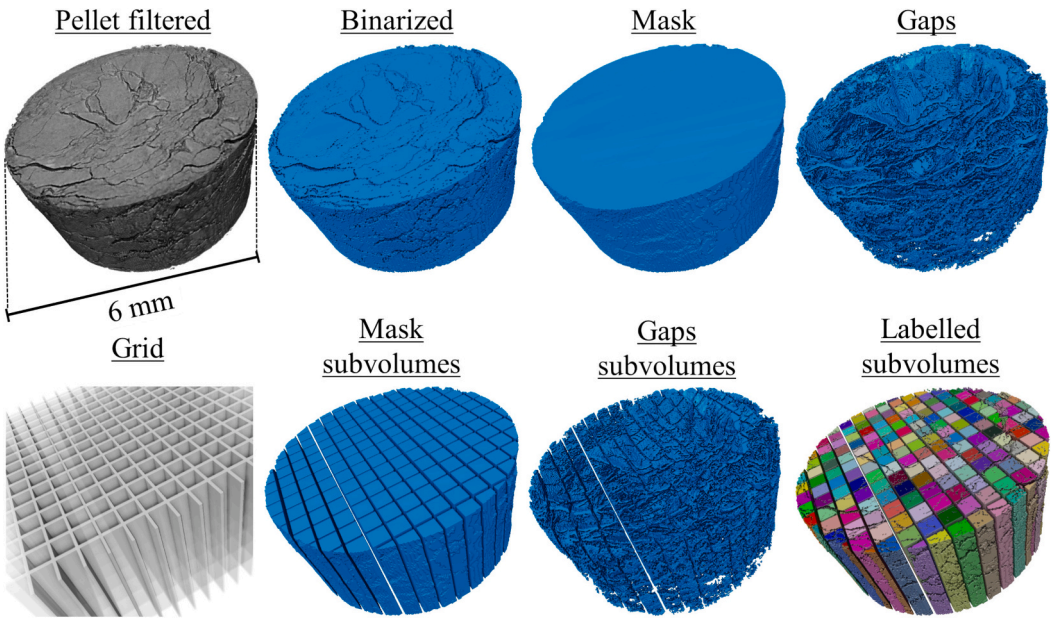

Fig. 2. Pellet section after non-local means filter (pellet filtered), binarization (binarized), masking (mask), binarization of the gaps (gaps), partitioning mask (mask subvolumes) and gaps (gaps subvolume) into subvolumes and creating pellet subvolumes (labelled subvolumes).

based on a sequence of "dilatation" and "erosion" steps with an intermediate "remove holes" step to close the voids inside the pellet. This allows to calculate the total volume of the pellet, as the resulting binary images show the outline of the wood (*Mask*, Fig. 2). By differentiating the binarized image from the pellet mask using the "arithmetic module", the outer air was separated from the inner air and the binary image of the gaps was obtained (*Gaps*, Fig. 2).

The **gap porosity (ε_{gaps})** was then calculated from the ratio of the pores (V_{gaps}) within the pellet to the volume of the pellet (V_{mask}):

$$\varepsilon_{gaps}\,[-] = \frac{V_{gaps}}{V_{mask}} \tag{5}$$

It should be noted that due to the limited spatial resolution, pores smaller than 6 μm are not considered in the gap porosity. To analyze the **radial distribution of the gap porosity**, another binary image of a grid containing subvolumes was created (*Grid*, Fig. 2). The size of the subvolumes within the grid should be as small as possible without affecting the estimation of the radial porosity. If the subvolumes are too small, they may contain only wood or pores, resulting in porosity values of either one or zero, leading to high scattered data. Too large subvolumes however would mask the local changes, especially the distinction between cracks on the surface and gaps between wood shavings. To ensure an adequate amount of data, while avoiding these issues, a size of 70x70x466 was selected for the suvolumes of the grid. The size was suitable for comparing pellets of great differences in their porosity. The length of 466 voxels in z direction was selected as it corresponds to the pellet length and leads to an additional reduction in the scatter, especially when considering smaller subvolumes at the periphery of the pellet.

The subtraction of the grid from the mask and the gaps results in the binary images *"gaps subvolumes"* and *"mask subvolumes"*, respectively. In the next step, all subvolumes of the pellet mask were assigned separate labels. Consequently, the gaps within each subvolume were assigned identical labels. By subtracting the *"gaps subvolumes"* from the *"mask subvolumes"*, subvolumes containing only labels representing wood phase was obtained (*labelled subvolumes*, Fig. 2). The porosity of each wood pellet subvolume ε_{SV} can then be determined as follows:

$$\varepsilon_{SV}\,[-] = 1 - \frac{V_{Labelled\ subvolume}}{V_{Mask\ subvolume}} \tag{6}$$

With the information about the barycenter *x* and barycenter *y* of each subvolume and the x coordinate (x_c) and y coordinate (y_c) of the pellet center, the radial distance (rd) of the subvolumes was determined:

$$rd = \sqrt{(x - x_c)^2 + (y - y_c)^2} \tag{7}$$

In the analysis of the radial distribution of the gap porosity, the average porosity within subvolumes located at comparable radial distances from the center was employed.

One way to estimate the **orientation of the gaps** is to examine the curvature of the two ends of the pellets. Such fracture ends are primarily caused by stresses on the wood pellets and are found at their weakest points with large gaps between wood shavings. For the μCT measurements, influencing factors such as additional stress and thus changes in the fracture ends due to transport must be excluded. Therefore, tensile stress was applied on seven unconditioned wood pellets to divide each of them into two halves obtaining 14 newly formed fracture ends. Subsequently, μCT measurements with a spatial resolution of 18 μm were performed on the 14 fracture ends (Fig. 3, left). Post-processing was carried out as previously described. The binarized fracture ends could be excised from the pellets by performing a line dilation of 10 px in the axial direction and differentiating the resulting image from the image before line dilation. In the next step, a binary image of a grid was used to divide each pellet end into subvolumes, as already done for the determination of the radial porosity distribution. Each subvolume of the grid had a voxel size of 70x70x466. To assess the **radial change of the height**, the radial distance of each subvolume was determined using their barycenter x and barycenter y according to eq. (7). The height of the individual subvolumes (barycenter z) was normalized to the height of the

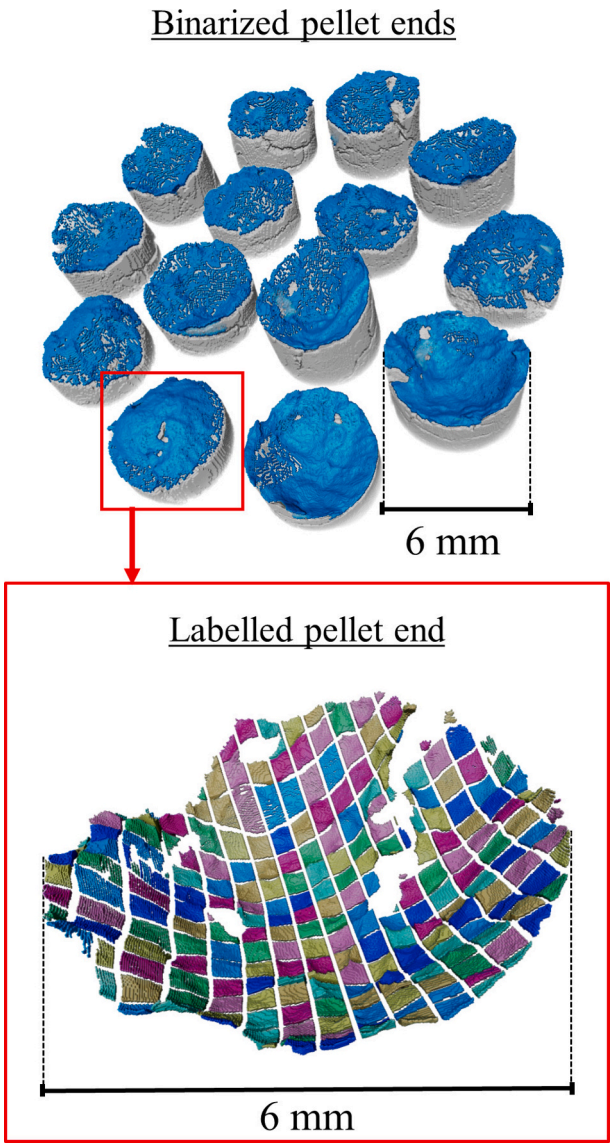

Fig. 3. Image of the binarized pellet ends (top) and illustration of the labelled subvolumes of a pellet end (bottom).

lowest subvolume. As the concave end and the convex end of the two halves of a pellet are identical, the average value of the height above the radius was determined from seven distinct convex ends.

2.7. Compression tests

2.7.1. Single wood pellet test

A total of 840 wood pellets (280 wood pellets of each type) were sanded to a uniform length as previously described. The 280 pellets of each type were divided into seven batches of 40 wood pellets. One batch represents the untreated wood pellets with a water content of 6–7 wt.-%. Three batches were humidified to water contents of approximately 10, 12 and 15 wt.-%, respectively. The remaining three batches were humidified to the same water contents and then re-dried to 6–7 w.-%. Each batch was further divided into 20 wood pellets for the axial compression test and 20 wood pellets for the diametrical compression test.

The **compression tests** were realized by using the Universal Testing Machine Series 1600 (ATS, USA) and the test speed was set at 0.5 mm/s. Before compression, the diameter and length of each pellet were measured according to DIN 863–1 [32]. The proportional stress limit (σ_P), strain (ε) and Young's modulus (E) were determined from the obtained force-displacement curves.

The proportional stress limit represents the stress at the end of the linear, elastic region and can be obtained from the corresponding force (F_P) and the load cross-section area (S_0) of the pellet as follows:

$$\sigma_P = \frac{F_P}{S_0} \tag{8}$$

with $S_{0,a} = \frac{\pi}{4} \bullet d_0^2$ for compression in axial direction and $S_{0,d} = \frac{d_0}{2} \bullet l_0$ assumed for compression in diametrical direction. Here, l_0 is the length and d_0 is the diameter of the pellet, respectively. The strain was calculated from the following equation:

$$\varepsilon_a = \frac{l}{l_0} \tag{9}$$

$$\varepsilon_d = \frac{d}{d_0} \tag{10}$$

with $\varepsilon_{a/d}$ for axial/diametrical compressive strain, l/d as length/diameter of the pellet at the corresponding force and l_0/d_0 as original length/diameter of the pellet. The Young's modulus E can be evaluated as the slope of the linear part of the stress-strain curve:

$$E = \frac{\Delta\sigma}{\Delta\varepsilon} \tag{11}$$

3. Results and discussion

3.1. Effect on pelleting parameters

Figure 4 illustrates the process conditions during the pelletization of pellets produced with press channel D/L ratios of 1:3, 1:4, and 1:5. With a channel diameter-to-length ratio of 1:3 (diameter = 6 mm / length = 18 mm), a specific energy consumption of 32 kWh/t, a temperature of 88 °C and a throughput of 50 kg/h were measured (Table 1). With a channel length up to 30 mm, a higher specific energy consumption of 104 kWh/t and a temperature of 103 °C resulted, while the throughput decreased to 25 kg/h. Here, the respective process parameters show a linear relationship with the channel length with $R^2 = 0.97$ for specific energy consumption, $R^2 = 0.96$ for temperature and $R^2 = 0.96$ for throughput.

Previous studies have shown that increasing the press channel length by keeping the diameter constant results in higher friction forces and higher back pressure towards the die inlet. Therefore, a greater energy

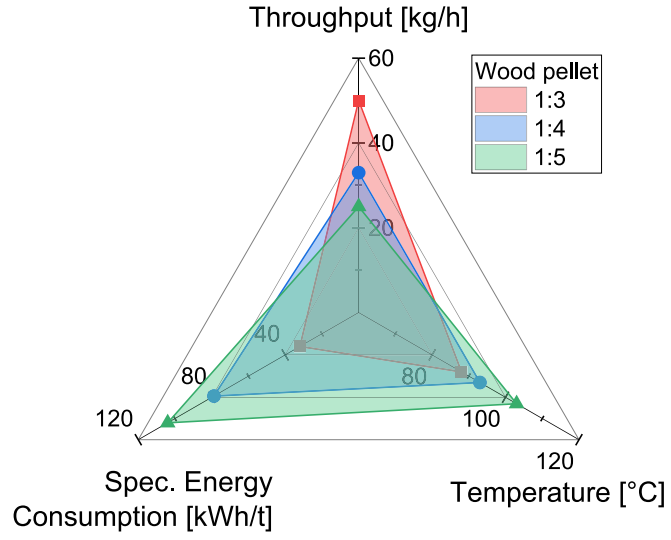

Fig. 4. Measured process parameters during the pelletization process of 1:3, 1:4 and 1:5 wood pellets.

Table 1
Measured data from the pelleting process.

Pellet type	Channel length	Througput	Temperature	Specific energy consumption
	[mm]	[kg/h]	[°C]	[kWh/t]
1:3	18	50	88	32
1:4	24	33	93	78.8
1:5	30	25	103	104

input by the roller is required to overcome the back pressure. Consequently, specific energy consumption rises and temperature increases, while the throughput is reduced with a longer press channel length (Table 1).

3.2. Effect on pellet structure and stability

The different process parameters resulting from the choice of die geometry also had a visual effect on the structure of the pellets. It can be seen that the 1:3 wood pellets retain their cylindrical shape but contain many cracks on the surface (Fig. 5). A shiny lignin layer, normally observed on the surface of pellets, was only partially present. During pelleting, it was also observed that some of the pellets had already broken off before reaching the cutting blade.

In contrast, the 1:4 pellets did not break off before the cutting blade and consist of significantly fewer cracks on their surface. The glossy lignin layer was observed on the surface of all of these pellets. The 1:5 pellets appear to have no visible cracks on their glossy surface. The first observations show that the choice of a die with a diameter (6 mm) to length (18 mm) ratio of 1:3 does not result in highly stable wood pellets. As the water content and particle size distribution of the wood shavings before pelleting were similar, they can be excluded as a possible reason for such differences. Since some of the raw wood shavings consisted of several smaller fragments that are held together by fine wood fibers, a reduction in wood shaving size during pelleting due to high mechanical loads was observed. However, the respective pellets 1:3, 1:4 and 1:5 consist of wood shavings with similar sizes (Fig. 6), i.e. the press channel length has no influence on the extent of comminution. Before pelleting, the wood shavings had a size of $x_{50.3}$ = 1218 µm (measured with the CamsizerXT) and after pelleting it decreased to 460–524 µm for wood

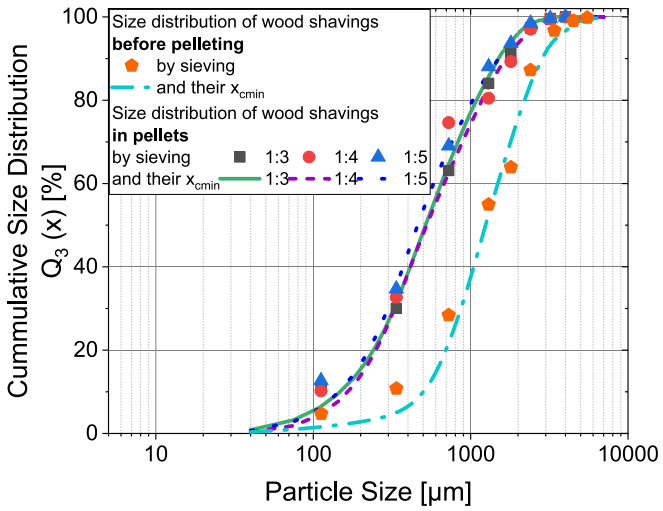

Fig. 6. Wood shaving size distribution before pelleting compared to wood shaving size distribution within pellets 1:3, 1:4 and 1:5 after pelletization.

shavings within the pellets 1:3, 1:4 and 1:5.

Since the wood shavings of all three pellet types were identical and pellets are known to have an open pore network, their true density does not differ significantly, too (Table 2). The apparent density $\rho_{app.}$ of 1.116 g/cm^3 and bulk density ρ_{Bulk} of 0.62 kg/dm^3 of 1:3 pellets are below the values required for the certificate A1 and B2 according to the standard DIN EN ISO 17225-2 (Table 2). In terms of these two parameters, both 1:4 and 1:5 pellets comply with the EN *plus A1* certificate. Corresponding to a linearly increasing density with a longer press channel from 18 to 30 mm with $R^2 = 0.988$, the total porosity decreases linearly with $R^2 = 0.986$. Here, 1:3 pellets have a total porosity of about 25 %, while 1:4 and 1:5 pellets show a total porosity of 22 % and 16 %, respectively. All the pellet types appear to be heterogeneous and show large deviations regarding their structural properties. The gap porosity of 1:4 pellets and 1:5 pellets do not differ to a high extent from each other, while the measured gap porosity of 1:3 are much higher. The gap porosity was determined using µCT data from three different wood pellets of each type (hereinafter referred to as M1, M2 and M3).

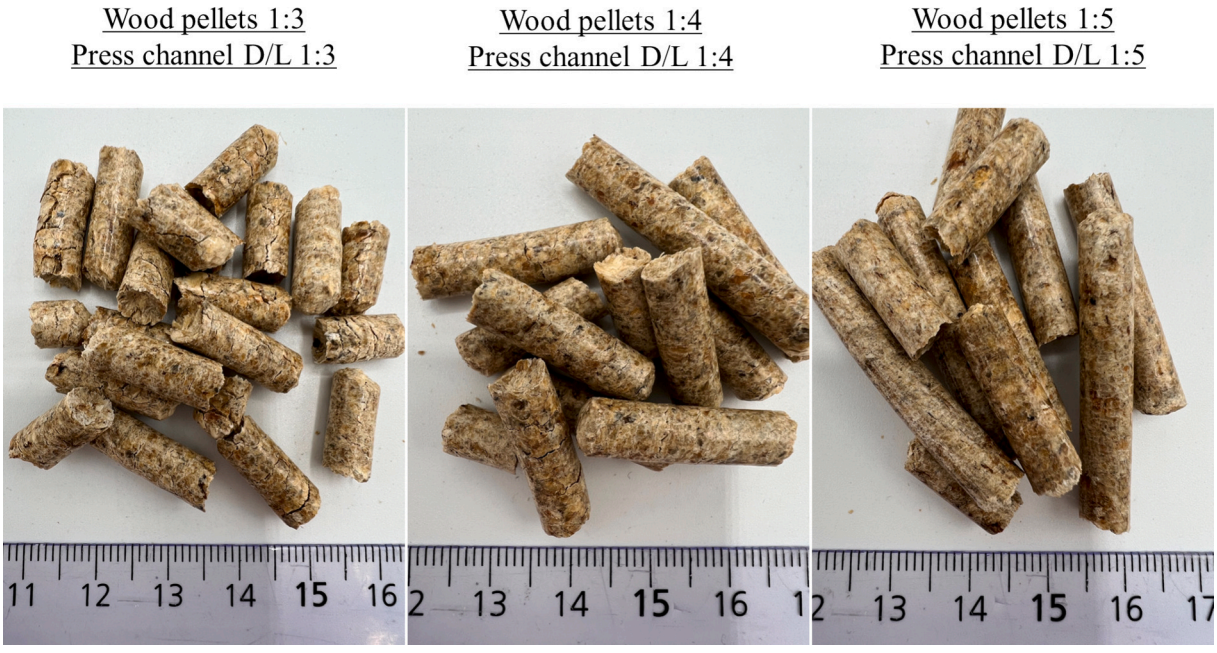

Fig. 5. Images of wood pellets 1:3, 1:4 and 1:5 after pelletization.

Table 2
Physical properties of wood pellets 1:3, 1:4 and 1:5.

Pellet type	–	1:3	1:4	1:5
Pellet diameter	[mm]	6.25 ± 0.07	6.2 ± 0.09	6.10 ± 0.03
Wood shavings $x_{50,3}$	[μm]	516	524	460
Water content	[wt.-%]	6.41	6.33	6.09
Gap porosity ε_{gaps} M1	[%]	11.68	5.98	5.01
Gap porosity ε_{gaps} M2	[%]	17.87	8.18	4.04
Gap porosity ε_{gaps} M3	[%]	13.16	6.46	3.99
Total porosity ε_{total}	[%]	25.35 ± 2.13	21.81 ± 3.11	16.47 ± 1.57
Apparent density $\rho_{app.}$	[g/cm^3]	1.160 ± 0.327	1.214 ± 0.484	1.293 ± 0.233
True density ρ_{true}	[g/cm^3]	1.456 ± 0.002	1.461 ± 0.002	1.447 ± 0.001
Bulk density ρ_{Bulk}	[kg/dm^3]	0.62	0.68	0.71

Since the wood shavings in all pellets have the same size distribution and the 1:5 pellets exhibit the highest apparent density, it can be assumed that 1:5 pellets consist of a higher number of accumulated wood shavings. Accordingly, a higher number of smaller gaps would result. However, some of the gaps are not visually apparent in the μCT images because of their smaller size than the spatial resolution of 6 μm (Fig. 7). In addition, the 1:5 pellets have a smaller diameter than the 1:4 and 1:3 pellets. It can be concluded that pellets produced under high stresses and thus higher die temperatures are less prone to relaxation after the cooling step leading to more gaps remaining in their small sizes. Nevertheless, it is the larger gaps that represent the greatest weak points for a pellet during mechanical stress. Sadeq et al. [38] showed that during a long-term storage under cyclic water content changes, a change in gap porosity (pores >6 μm) correlates very well with a change in mechanical strength. In this study, both the distribution of the gap porosity in the radial direction of a pellet and the U-shape form of the gaps resulting from the conical inlet during pelleting appear to change as a function of the press channel length. In the case of 1:3 pellets made with a channel length of 18 mm, the wood shavings and thus the gaps seem to be more aligned in the longitudinal direction compared to 1:4 and 1:5 wood pellets (Fig. 7).

The alignment of the gaps was approximated from the analysis of the alignment of the fracture end of a pellet as described in section 2.4. The fracture ends result from mechanical stress, especially at the points of a pellet with larger gaps [38]. From the 3D representation of the convex fracture ends in Fig. 8, it becomes clear that the lowest point is not always located in the center of the pellet. The points along the circumference of the pellet vary in their height, too. Compared to studies in which the shape of the layers was examined using a 2D image, the analysis of the height over the radius from 3D data results in a larger standard deviation. These large deviations can be explained by a broad size distribution of the wood shavings and the dynamic conditions during pelleting leading to uneven fracture ends.

Despite the large deviation, however, the height over the normalized

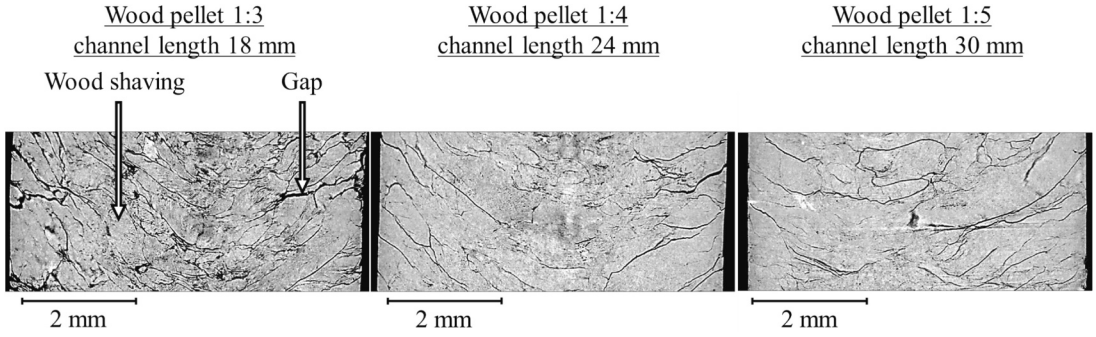

Fig. 7. Longitudinal cross cut of a section of 1:3, 1:4 and 1:5 wood pellet from μCT measurements.

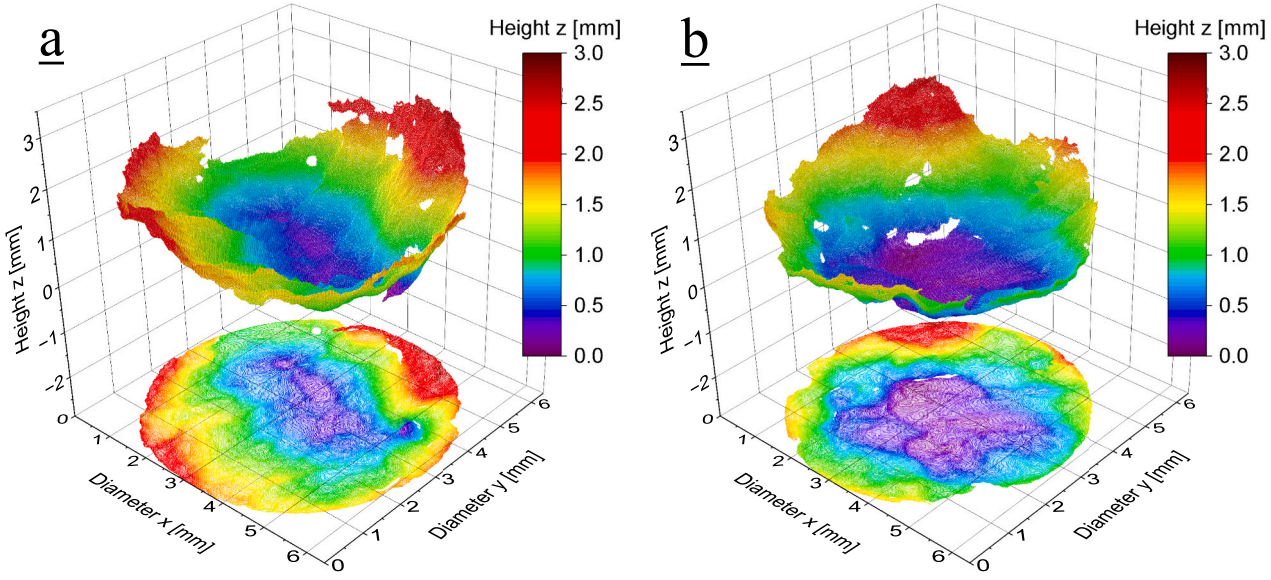

Fig. 8. 3D representation of 1:3 pellet convex end (a) and 1:5 pellet convex end (b).

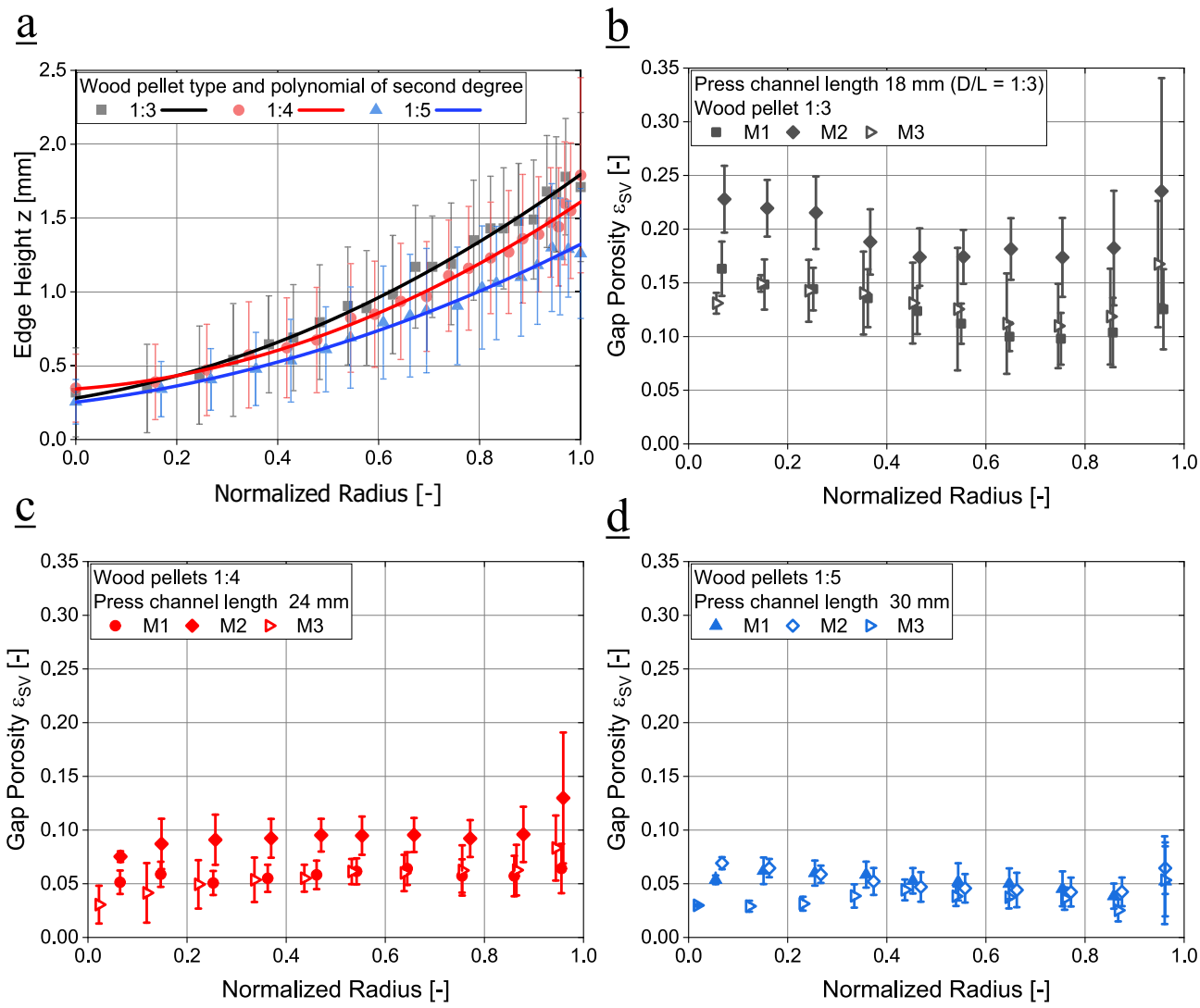

Fig. 9. Height of the pellet convex end along the normalized pellet radius (a) and radial distribution of the gap porosity of wood pellet type 1:3 (b), 1:4 (c) and 1:5 (d) pellets measured three times (M1-M3).

radius can be described with a polynomial of second degree (Fig. 9a). Here, a clearer difference in the height between 1:3, 1:4 and 1:5 pellets can be observed near the pellet surface.

Dies with a longer press channel are known to lead to a higher wall friction resulting in higher die temperature and adhesion forces. Reaching a required minimum temperature in the entire press channel could also lead to uniform softening of wood and binding components enabling a better compactibility and thus a more uniform back pressure. The reduced relaxation of pellets after the cooling step leads to 1:4 and 1:5 pellets exhibiting a uniform density and porosity distribution along the pellet radius (Fig. 9c and d). In contrast, a high gap porosity in the center of 1:3 wood pellets can be explained by low accumulation of particles within the press channel of a length of 18 mm (Fig. 9). Here, a low temperature in the center of the press channel as described in the literature [14] may not ensure sufficient softening of the wood components resulting in bigger pellets with lower relaxed density. From the μCT image of the longitudinal cross cut of the 1:3 pellet (black lines in Fig. 7), it can be seen that higher gap porosity near the pellet surface is due to cracks propagating towards the center. The wood shavings are shown in light gray due to their higher density than the gaps consisting of air (black). A dark gray region in the center of the pellet results from more single pores between the wood shavings explaining the higher value of gap porosity in Fig. 9b. In contrast, the 1:4 pellet shows a smaller difference in gray values along the radial direction, and no difference can be observed visually for the 1:5 pellet (Fig. 7), which is in accordance to their uniform gap porosity distribution shown in Fig. 9c, d. While there are distinct variations in the gap porosity profile across the radius between different pellet types, there are also noticeable discrepancies in porosity levels among the three measurements of the same pellet type, likely due to inherent heterogeneity.

After pelleting, high density pellets show a high proportional stress limit (PSL) σ_P (Table 3). From the force-displacement data, an initial longer compression phase was observed for the porous 1:3 pellets than for the less porous 1:4 and 1:5 pellets. However, the lower proportional

Table 3
Mechanical stability of wood pellets 1:3, 1:4 and 1:5.

Wood pellet	Axial PSL σ_P [MPa]	Young's Modulus E (axial) [MPa]	Diametral PSL σ_P [MPa]	Young's Modulus E (diametral) [MPa]
1:3	7.40 ± 0.98	101 ± 35	7.91 ± 1.34	108 ± 81
1:4	17.42 ± 3.87	321 ± 113	14.15 ± 2.66	164 ± 34
1:5	24.17 ± 4.21	561 ± 116	20.49 ± 2.32	261 ± 75

stress limit in both load directions indicates that the 1:3 pellets are significantly less stable. In comparison, the stiffness and PSL of 1:4 and 1:5 wood pellets are significantly higher. A linear relationship was found when considering PSL and the press channel length of the dies used for the production of the respective pellet types (Table 3). This applies to both the axial PSL ($R^2 = 0.987$) and the diametrical PSL ($R^2 = 1$). While diametrical PSL was found to be higher than axial PSL in other studies [38], only minor difference were observed here. Many influencing factors, such as the size distribution of the shavings and whether they are arranged more in the longitudinal or radial direction of the pellets can lead to these strong differences in the PSL.

The extent to which mechanical properties of the pellets change during storage with fluctuating relative humidity is discussed in the following.

3.3. Structure and stability at wet state

The sorption isotherms of wood pellets investigated in this study follow a sigmoidal shape and correspond to type II isotherms according to van der Waal, which agrees to the literature. Since the pellets consist of the same raw material, there are only slight differences in their sorption isotherms and in the maximum water content. These slight differences may arise due to the heterogeneity of the wood pellets. A comparison with sorption isotherms from literature [37,50–54] shows that the maximum water content of wood pellets from different tree species can vary greatly. For example, [37] showed that commercial wood pellets made from spruce and a mixture of softwood and hardwood have a water content of around 12 wt.-% at 90 % relative humidity, while the maximum water content of the wood pellets examined in this study is about 15 wt.-% (Fig. 10). After the subsequent desorption of water vapor, a hysteresis, which is assumed to be the result of the "ink bottle effect", is formed.

It has been reported that spruce and mixed pellets swell only moderately in the longitudinal direction with increasing water content. In comparison, a larger percentage increase in pellet length and therefore pellet volume was observed for the wood pellets in this study. The higher swelling in the longitudinal and radial direction at a water content of 12.5 wt.-% leads to a volume increase of about 20–30 % (Fig. 10), while in [37] a volume increase of about 15 % was reported for spruce and mixed pellets. Additionally, in contrast to their linear increase in volume up to a water content of 12 wt.-%, an exponential trend can be seen for 1:3, 1:4 and 1:5 wood pellets.

Although the initial density and stability of the wood pellets in this study are within the range of some untreated wood pellets from literature, they can undergo a significantly greater change in structure during storage at high humidity. The varying behavior of the wood pellets may be attributed to the origin of the wood shavings as well as material and process conditions during pelleting. The wood pellets in this study were produced using a flat die press, while the commercial spruce and mixed pellets from [37] were produced with a ring die press. Further information about their pelleting conditions were not available in the literature. However, a common characteristic of wood pellets is their excessive volume enlargement when the saturation vapor pressure is exceeded by using the ultrasonic humidifier in the climate chamber. Here, a resulting higher water absorption rate leads to a water content of >12 wt.-% and greater structural damage to the wood pellets. The greater damage showed up in a visibly higher number of wider and deeper cracks on the pellet surface. Thus, the change in apparent pellet density, degree of saturation (Fig. 11) and total porosity (Fig. 13a) is consistent with the findings of previous studies. An initial increase in pellet density and degree of saturation occurs as water is adsorbed by the wood shavings. However, exceeding the saturation vapor pressure and the associated excessive swelling of the pellet results in smaller proportion of voids filled with water. As a consequence, the apparent pellet density and degree of saturation drop from a water content of >12 wt.-%. On the other hand, the total porosity increases continuously due to the enlarged pores of the swollen wood shavings and the growing cracks (Fig. 13a). The degree of saturation shows a distinct contrast between

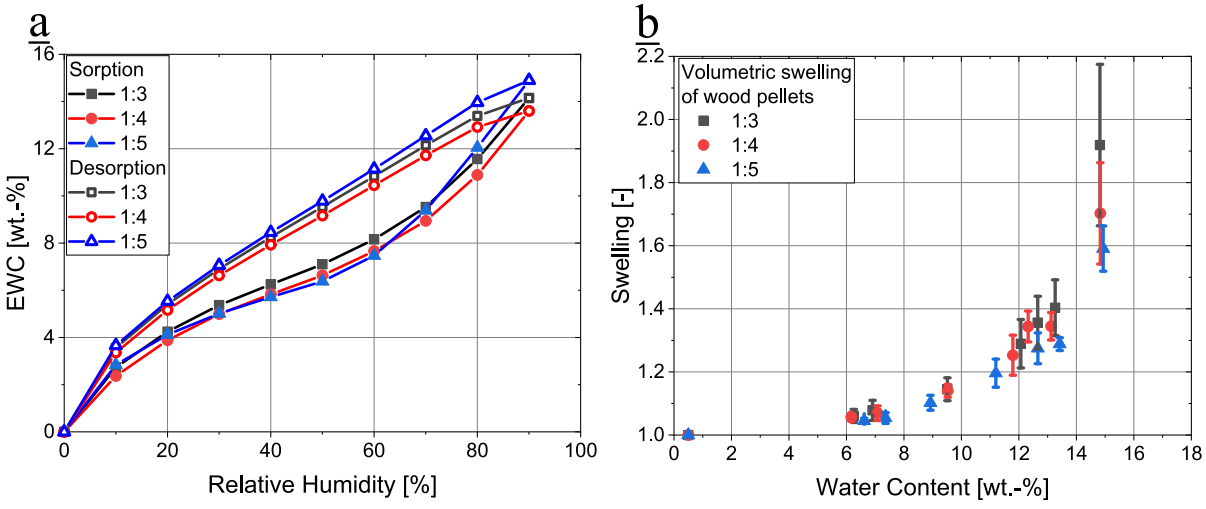

Fig. 10. Sorption isotherms (a) and swelling characteristics (b) of wood pellets 1:3, 1:4 and 1:5 with increasing water content.

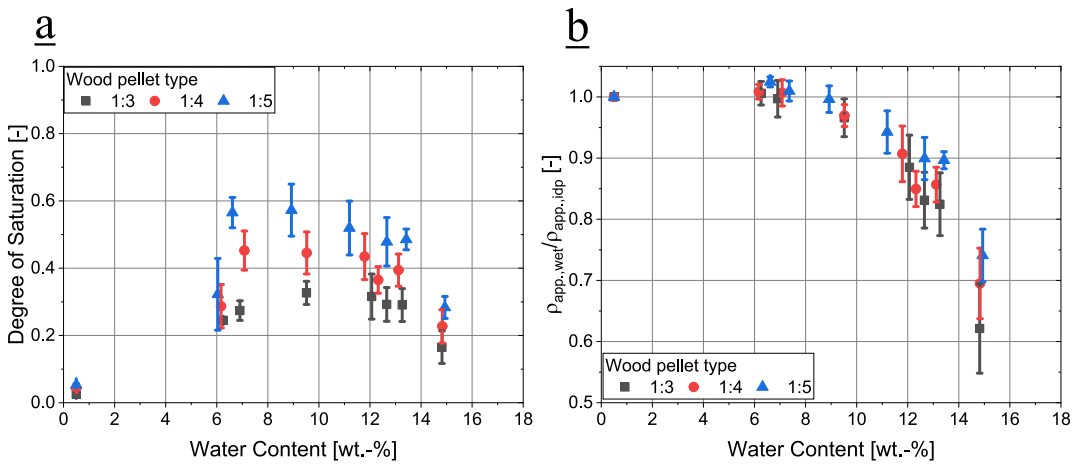

Fig. 11. Degree of saturation (a) and changes in the apparent density (b) of wood pellets at higher water content.

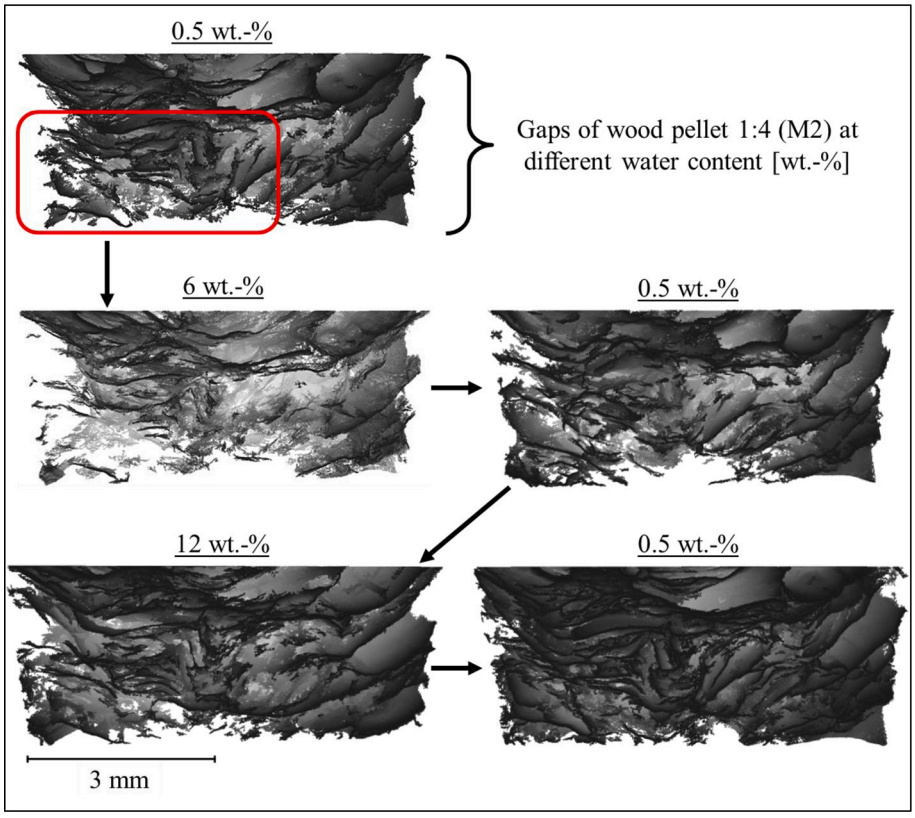

Fig. 12. Images of the longitudinal cross cut of gaps (dark colored) of a 1:4 wood pellet at its initial dry state, wet state and re-dried state.

high-density and low-density pellets as the high density 1:5 pellets exhibit a more pronounced increase, reaching a higher maximum value. Despite the swelling of the pellets and expanding of their total void volume at increasing water content, the proportion of water-filled pores is much greater in compact pellets with lower initial total void volume.

The total void volume of a pellet considers the gaps and the pores of the wood shavings. As the water content increases, a change in the internal structure can be observed (Fig. 12).

Here, images of the longitudinal cross cut obtained from μCT scans of a wood pellet (wood pellet 1:4, M2, Fig. 9) in its initial dry state and subsequently ranging different water contents are shown. Humidification and re-drying to achieve the desired water contents were carried out one after the other. It can be seen, that, with an increase of the water content from 0.5 to 6 wt.-%, the average size of the gaps become smaller as the wood shavings swell and fill the gaps. Some visible gaps in the initial dry state (marked in red, Fig. 12) that decreased to a size below the spatial resolution of 6 μm, are absent in the image at a water content of 6 wt.-%. This was also the case with the 1:3 and 1:5 pellets. Although

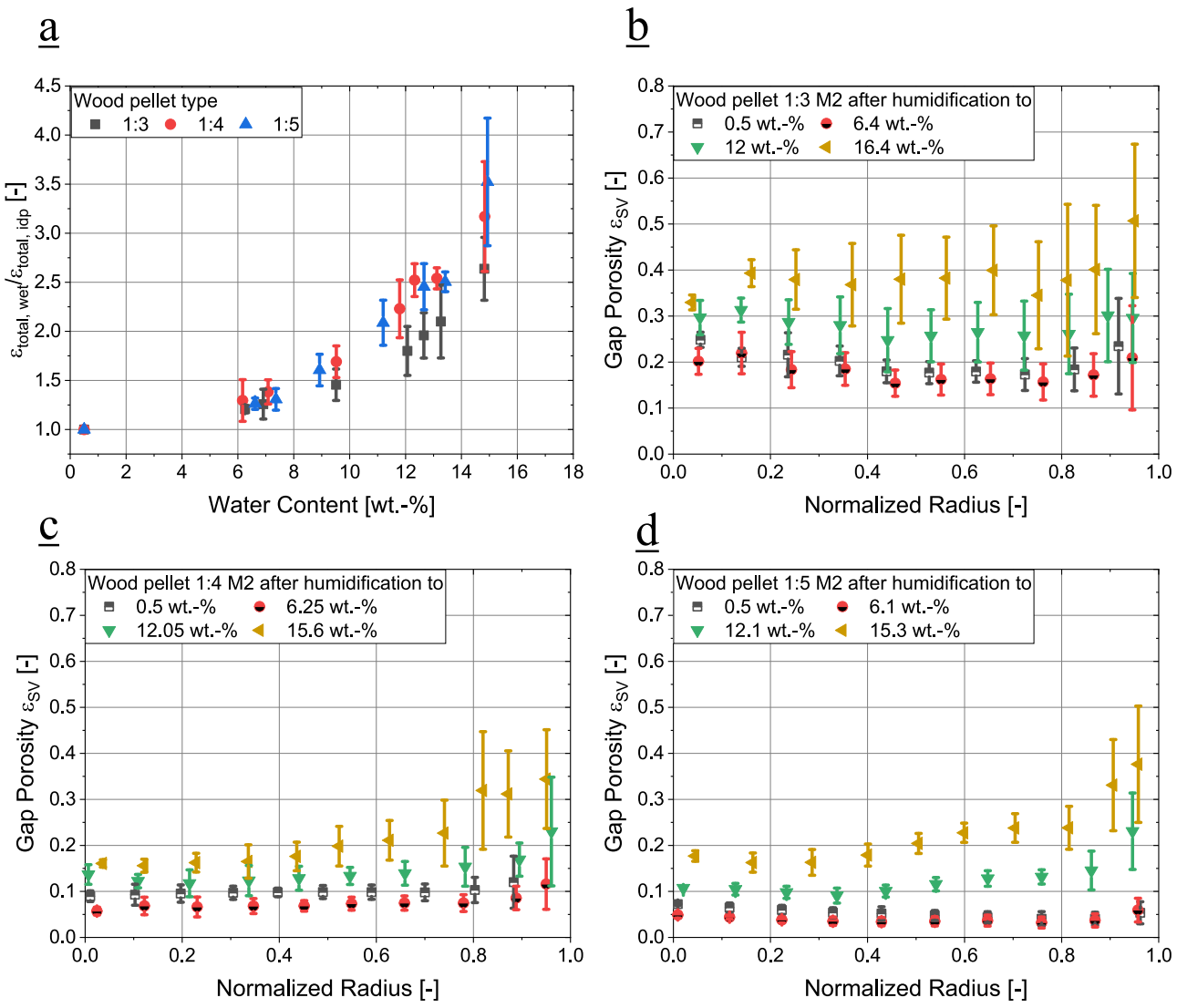

Fig. 13. Changes in total porosity at higher water content (a) and changes in the gap porosity over the normalized pellet radius of 1:3 (b), 1:4 (c) and 1:5 (d) wood pellets at increasing water content.

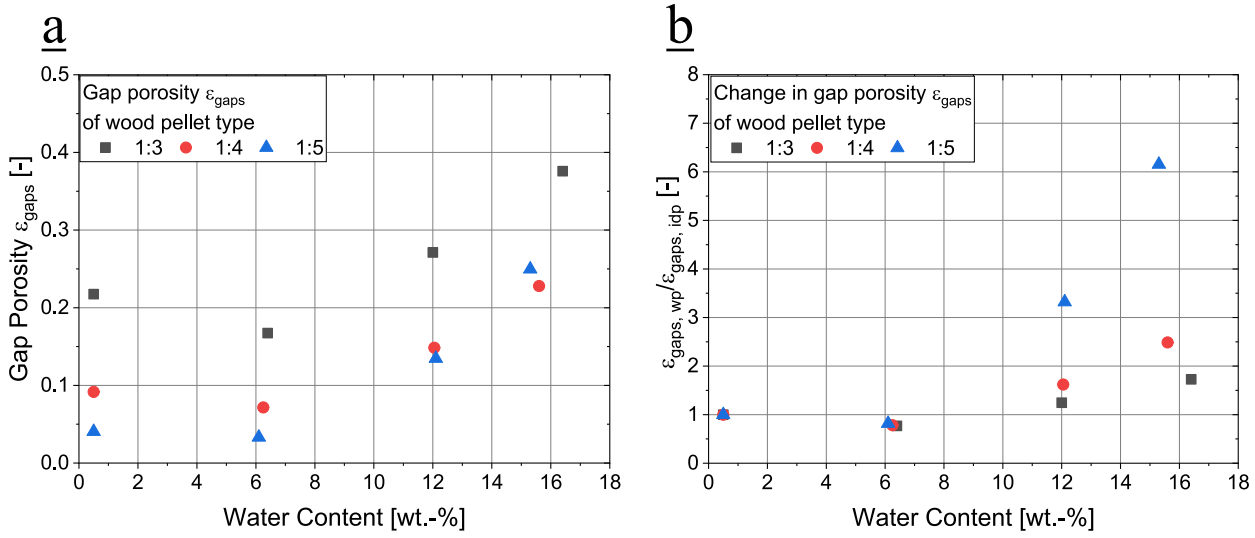

Fig. 14. Changes in gap porosity at increasing water content (a) and ratio of the gap porosity of wet pellets and initial dry pellets (b).

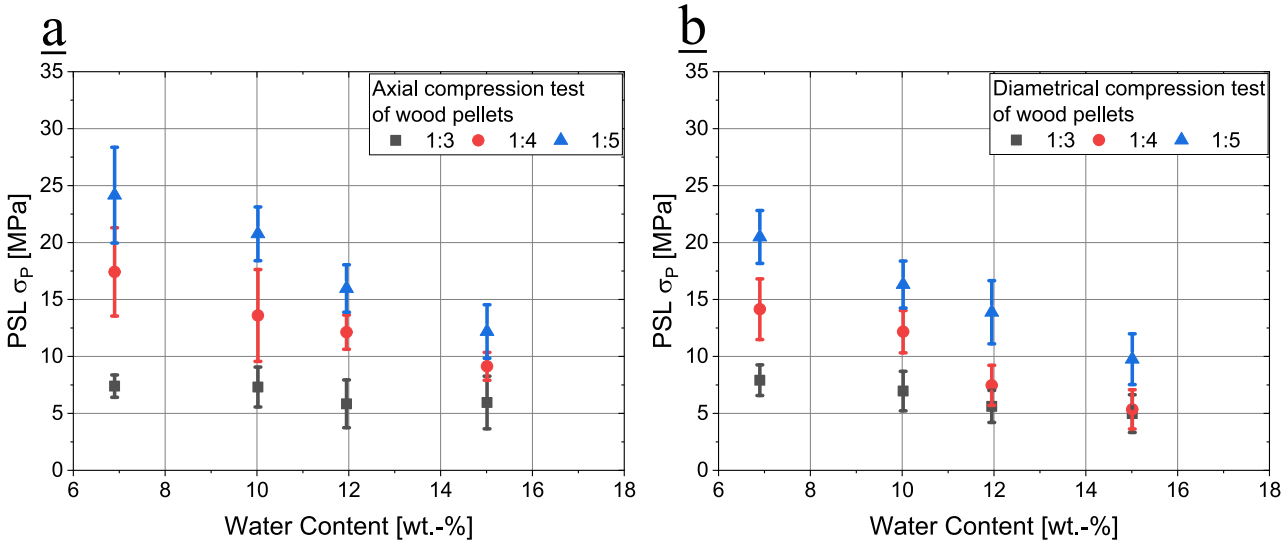

Fig. 15. Axial PSL (a) and diametral PSL (b) of wood pellets 1:3, 1:4, 1:5 at increasing water content.

the radial gap porosity distribution shifts to smaller values (Fig. 13b-d), the total porosity (Fig. 13a) rises due to increased bigger pores of the swollen wood shavings and the overall enlarged pellet volume. However, the shape of the distribution curve of the radial gap porosity at a water content of about 6 wt.-% does not exhibit significant differences compared to the distribution curve of the pellet's initial dry state. In contrast, at water contents exceeding 12 wt.-%, the distribution of the gap porosity becomes less homogeneous. This is primarily attributed to a greater number of larger cracks on the pellet surface, resulting in a locally higher gap porosity. In addition, uneven changes occurring at regions with the same radial distance from the pellet center, lead to large deviations. The structural degradation of wood pellets appears to continue inwards as the water content increases. Thus, for all wood pellets at a water content of >15 wt.-%, a significant rise of the gap porosity can be observed in the pellet center.

Although 1:3 wood pellets consist of bigger pores at higher water contents, a larger percentage change in the gap porosity can be observed for high density 1:4 and 1:5 wood pellets (Fig. 14b). Accordingly, the ratio of the total porosity (Fig. 13a) in the wet state to the untreated state (6–7 wt.-%) is greater for 1:4 and 1:5 pellets than for low density 1:3 pellets. The extent to which wood pellets change during humidification can be related to the conditions set during the pelleting process. With longer press channels, a temperature of >90 °C (Table 1) during pelleting lead to uniform softening of the wood components throughout the press channel resulting in homogeneous compaction of wood shavings and thus a uniform radial porosity distribution, as with 1:4 and 1:5 pellets (Fig. 13).

During cooling, the binding components can quickly transition back to their glassy state. The springback effect is reduced and the pellets do not expand as much as would be the case without the cooling step. However, this preserved structure cannot be maintained throughout, as the binding components like lignin begin to soften again during storage at high humidity. With an increase of the molecular mobility of lignin, high-density wood pellets may undergo a greater proportionate structural change (Fig. 13, Fig. 14b). In contrast, the high radial porosity of untreated 1:3 pellets (Fig. 9) and a die temperature of <90 °C (Table 1) indicate lower adhesion forces between the wood shavings during pelleting and a stronger springback effect. Therefore, due to the greater surface contact between the wood shavings in 1:4 and 1:5 wood pellets, the expected higher adhesion can show up in a higher mechanical stability. This can be seen in the PSL despite the humidification of wood pellets from a water content of 7 to a critical water content of 10 wt.-% as defined by the DIN standard. Here, the 1:4 and 1:5 wood pellets are significantly more stable in their axial and diametral PSL compared to the 1:3 wood pellets (Fig. 15). This also shows that both the softening of the binding components and a required minimum level of structural damage are responsible for the reduction in stability. It is noteworthy that the PSLs of the different pellet types approach each other as the water content increases. The higher stability of the 1:4 and 1:5 even at high water contents is attributed to increased adhesion forces resulting from a larger contact area between the wood shavings. However, it is expected that this difference diminishes when the water content exceeds 15 wt.-% and structural damage to the wood pellets 1:4 and 1:5 becomes more pronounced.

Despite the decrease of mechanical strength and structural damage at high water contents, wood pellets have the potential to recover when desorbing water at subsequent low humidity.

In comparison to the wet state (Fig. 13a), after re-drying, the total porosity has decreased due to the shrinkage of the shavings (Fig. 16a). Accordingly, the volume and density of re-dried wood pellets are smaller compared to their previous wet state. Although the pellets appear to have recovered in their structure to some extent, there are still major differences to their initial dry state. Shrinkage of the wood shavings resulted in larger gaps and slightly higher radial gap porosity (Fig. 16b-c) when comparing to their initial dry state. Here, the pattern of radial gap porosity resembles that of the respective pellets in their wet state, indicating that large cracks formed in the wet state persist in the re-dried state. Therefore, wood pellets cannot recover fully as remaining damages after one humidification and re-drying cycle are present in the form of these larger gaps.

The expanded gaps between the wood shavings result in pellets with a higher diameter and length compared to their initial dry state and prevent the wood pellet from regaining its original volume or density (Fig. 17).

By reducing the water content, lignin transitions from its rubbery state back to its glassy state and wood pellet stability will rise again. To

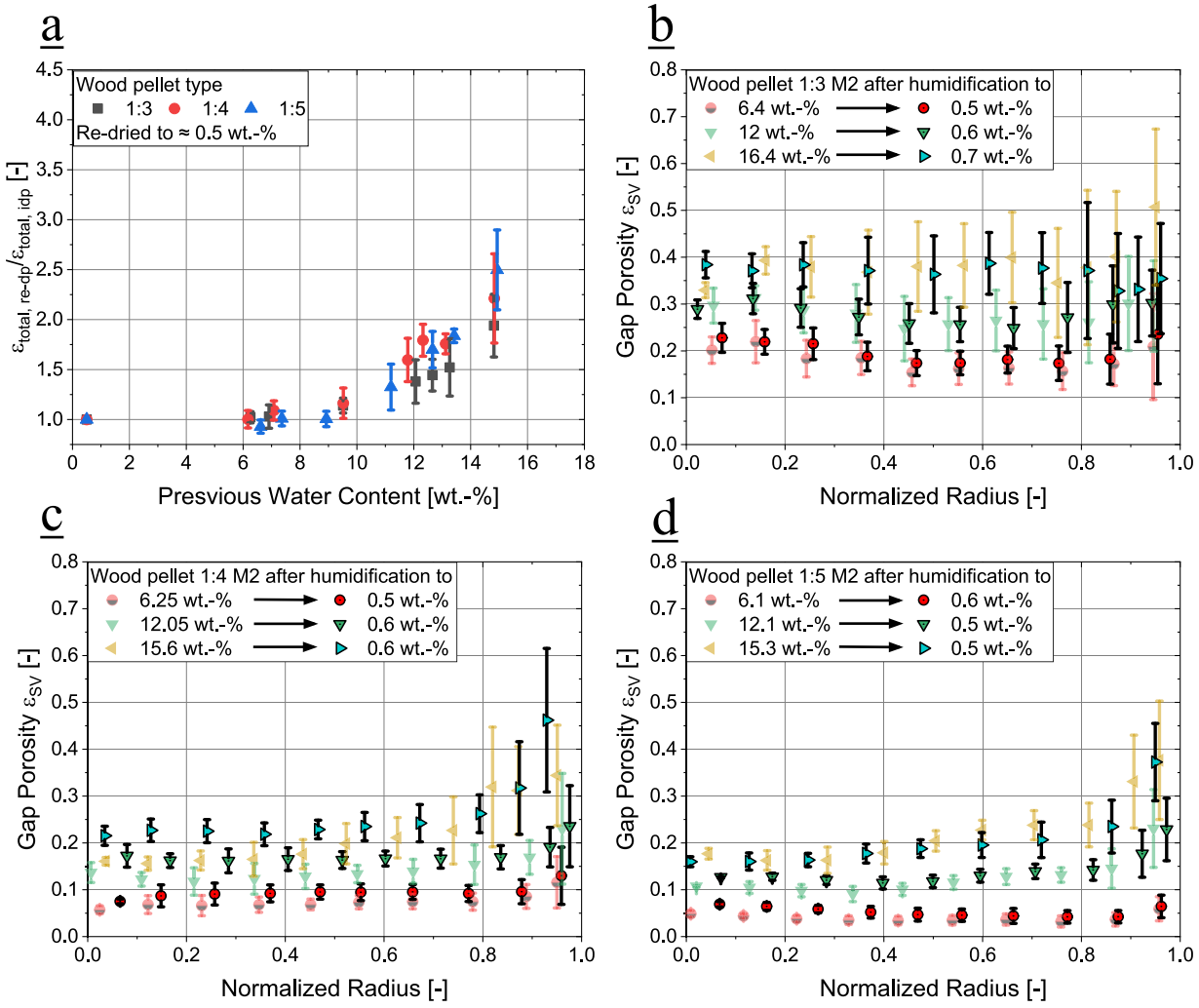

Fig. 16. Changes in total porosity (a) and radial gap porosity of 1:3 (b), 1:4 (c) and 1:5 (d) pellets.

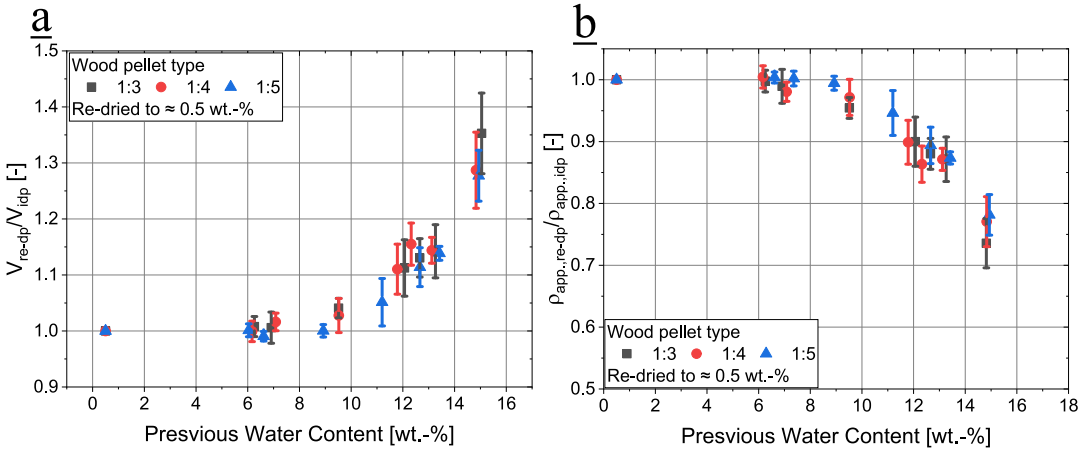

Fig. 17. Comparison of the volume (a) and density (b) of re-dried pellets with their initial dry state.

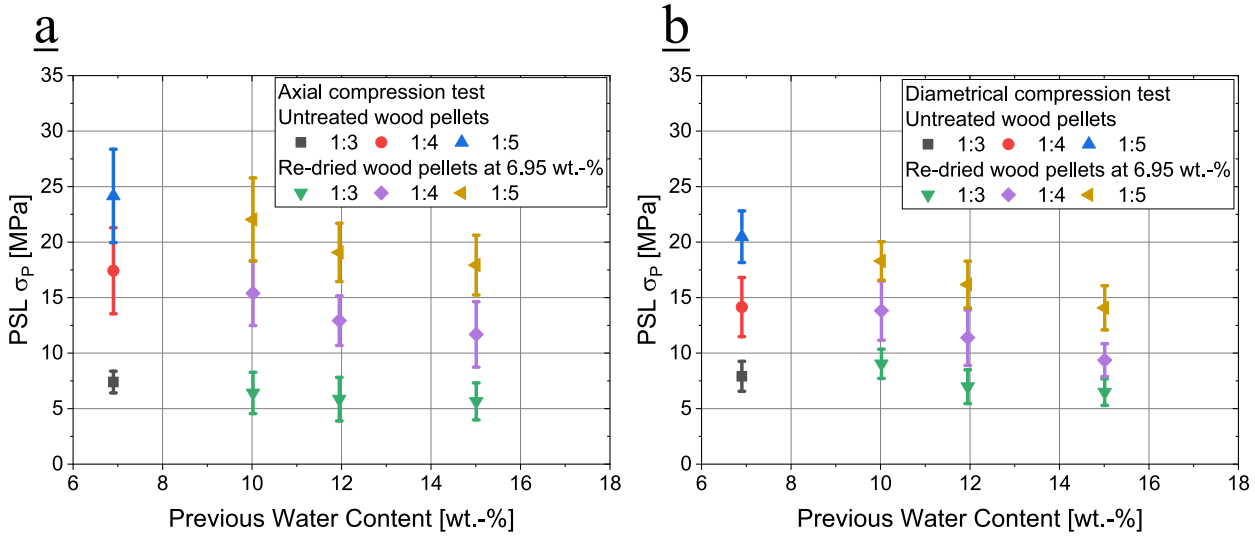

Fig. 18. Comparison of the axial PSL (a) and diametral (PSL) (b) of re-dried wood pellets with their untreated state.

investigate this, wet pellets were re-dried to the same water content as in the case of their untreated state (approx. 6–7 wt.-%). Here the extent to which the wood pellets can recover in their stability seems to depend on their initial properties and their water content in the wet state (Fig. 18).

For example, re-dried 1:5 wood pellets with a previous water content of 15 wt.-% appear to have recovered the most by 47 % in their axial PSL and 44 % in their diametral PSL. This is due to the fact that the 1:5 pellets at 15 wt% exhibited significantly lower gap porosity and consequently less structural damage compared to the other pellet types (Fig. 16). As a result, the higher stability of re-dried 1:5 wood pellets arises from an increased contact area between the wood shavings.

4. Conclusions

The study highlights the significant role of press channel geometry, providing valuable insights into interacting parameters such as temperature and back pressure, which affect wood pellet quality at delivery state and during storage. The wood pellet quality was evaluated, focusing on density, structural integrity, and radial porosity distribution and mechanical stability. Key findings include:

- Process efficiency: Longer press channels (1:4 and 1:5 D/L ratios) require more energy and result in higher die temperatures but lower production throughput compared to shorter channels (1:3 ratio).
- Pellet quality: Wood pellets from longer press channels exhibit higher density and fewer surface cracks, indicating better compaction and structural stability.
- Radial porosity: Wood pellets from longer press channels show more uniform radial porosity and lower gap porosity, suggesting more consistent compaction and reduced internal gaps.
- Mechanical stability: Higher strength and stiffness are observed in wood pellets from longer press channels, reflecting improved mechanical properties and better resistance to structural damage.
- Humidity resistance: Wood pellets from longer press channels maintain better structural integrity and exhibit less swelling and gap increase under high humidity conditions compared to those from shorter press channels. Structural damages due to high humidity due to surface crack propagating inwards.
- Recovery: High-density pellets recover more effectively in mechanical strength and structural integrity after re-drying compared to low-density pellets. Remaining damages are present in the form of bigger gaps between wood shavings in the wood pellets.

In summary, wood pellets produced with a longer press channel exhibit enhanced resistance to mechanical loads, resulting in reduced fines generation during transport. Additionally, high-density pellets demonstrate reduced structural damage when subjected to humidity fluctuations, indicating improved storage stability. Future research should investigate the long-term effects of multiple humidity cycles on pellet stability and evaluate the associated cost implications.

CRediT authorship contribution statement

Abdullah Sadeq: Writing – review & editing, Writing – original draft, Visualization, Validation, Methodology, Investigation, Formal analysis, Data curation, Conceptualization. **Swantje Pietsch-Braune:** Writing – review & editing. **Stefan Heinrich:** Writing – review & editing, Supervision, Resources, Project administration, Funding acquisition.

Declaration of competing interest

The authors declare that they have no known competing financial interests or personal relationships that could have appeared to influence the work reported in this paper.

Data availability

Data will be made available on request.

Acknowledgement

The authors would like to thank for the funding of this research by the German Research Foundation (Deutsche Forschungsgemeinschaft, DFG) in the framework of Research Training Group GRK2462-Project No. 390794421: Processes in natural and technical Particle Fluid Systems (PintPFS) [DFG PintPFS, 2019] at Hamburg University of Technology (TUHH). The authors would also like to thank Amandus Kahl GmbH & Co. KG and Power Pellets GmbH & Co. KG for their useful comments during this project. Publishing fees supported by Funding Programme Open Access Publishing of Hamburg University of Technology (TUHH).

References

[1] R. Luque, L. Herrero-Davila, J.M. Campelo, J.H. Clark, J.M. Hidalgo, D. Luna, et al., Biofuels: a technological perspective, Energy Environ. Sci. 1 (2008) 542–564, https://doi.org/10.1039/B807094F.

[2] S.K. Nielsen, M. Mandø, A.B. Rosenørn, Review of die design and process parameters in the biomass pelleting process, Powder Technol. 364 (2020) 971–985, https://doi.org/10.1016/j.powtec.2019.10.051.

[3] J. Dai, J.R. Grace, Biomass granular screw feeding: an experimental investigation, Biomass Bioenergy 35 (2011) 942–955, https://doi.org/10.1016/j.biombioe.2010.11.026.

[4] J.S. Tumuluru, C.T. Wright, J.R. Hess, K.L. Kenney, A review of biomass densification systems to develop uniform feedstock commodities for bioenergy application, Biofuels Bioprod. Biorefin. 5 (2011) 683–707, https://doi.org/10.1002/bbb.324.

[5] X. Zhou, X. Li, Z. Cui, L. Wu, H. Zhou, X. Lu, Combustible wood dust explosions and impacts on environments and health - a review, Environ. Res. 216 (2023) 114658, https://doi.org/10.1016/j.envres.2022.114658.

[6] N. Kaliyan, Morey R. Vance, Factors affecting strength and durability of densified biomass products, Biomass Bioenergy 33 (2009) 337–359, https://doi.org/10.1016/j.biombioe.2008.08.005.

[7] M.T. Carone, A. Pantaleo, A. Pellerano, Influence of process parameters and biomass characteristics on the durability of pellets from the pruning residues of *Olea europaea* L, Biomass Bioenergy 35 (2011) 402–410, https://doi.org/10.1016/j.biombioe.2010.08.052.

[8] M. Temmerman, F. Rabier, P.D. Jensen, H. Hartmann, T. Böhm, Comparative study of durability test methods for pellets and briquettes, Biomass Bioenergy 30 (2006) 964–972, https://doi.org/10.1016/j.biombioe.2006.06.008.

[9] DIN EN ISO 17225-2:2021-09, Biogene Festbrennstoffe_- Brennstoffspezifikationen und -klassen_- Teil_2: Klassifizierung von Holzpellets (ISO_17225–2:2021); Deutsche Fassung EN_ISO_17225–2, 2021, https://doi.org/10.31030/3215000 n.d.

[10] N. Kaliyan, R.V. Morey, Natural binders and solid bridge type binding mechanisms in briquettes and pellets made from corn Stover and switchgrass, Bioresour. Technol. 101 (2010) 1082–1090, https://doi.org/10.1016/j.biortech.2009.08.064.

[11] C. Salas-Bringas, T. Filbakk, G. Skjevrak, O.-I. Lekang, O. Høibø, R. Schüller, Compression rheology and physical quality of wood pellets pre-handled with four different conditions, Ann. Transact. Nordic Rheol. Soc. 18 (2010) 87–93.

[12] E.L. Back, The Bonding Mechanism in Hardboard Manufacture Review Report, Holzforschung 41 (1987) 247–258, https://doi.org/10.1515/hfsg.1987.41.4.247.

[13] P. Gilbert, C. Ryu, V. Sharifi, J. Swithenbank, Effect of process parameters on pelletisation of herbaceous crops, Fuel 88 (2009) 1491–1497, https://doi.org/10.1016/j.fuel.2009.03.015.

[14] C. Serrano, E. Monedero, M. Lapuerta, H. Portero, Effect of moisture content, particle size and pine addition on quality parameters of barley straw pellets, Fuel Process. Technol. 92 (2011) 699–706, https://doi.org/10.1016/j.fuproc.2010.11.031.

[15] J.K. Holm, U.B. Henriksen, J.E. Hustad, L.H. Sørensen, Toward an Understanding of Controlling Parameters in Softwood and Hardwood Pellets Production, Energy Fuel 20 (2006) 2686–2694, https://doi.org/10.1021/ef0503360.

[16] J.K. Holm, U.B. Henriksen, K. Wand, J.E. Hustad, D. Posselt, Experimental verification of novel pellet model using a single pelleter unit, Energy Fuel 21 (2007) 2446–2449, https://doi.org/10.1021/ef070156l.

[17] S. Mani, L.G. Tabil, S. Sokhansanj, Effects of compressive force, particle size and moisture content on mechanical properties of biomass pellets from grasses, Biomass Bioenergy 30 (2006) 648–654, https://doi.org/10.1016/j.biombioe.2005.01.004.

[18] M.D. Shaw, C. Karunakaran, L.G. Tabil, Physicochemical characteristics of densified untreated and steam exploded poplar wood and wheat straw grinds, Biosyst. Eng. 103 (2009) 198–207, https://doi.org/10.1016/j.biosystemseng.2009.02.012.

[19] I. Relova, S. Vignote, M.A. León, Y. Ambrosio, Optimisation of the manufacturing variables of sawdust pellets from the bark of *Pinus caribaea* Morelet: Particle size, moisture and pressure, Biomass Bioenergy 33 (2009) 1351–1357, https://doi.org/10.1016/j.biombioe.2009.05.005.

[20] D. Bergström, S. Israelsson, M. Öhman, S.-A. Dahlqvist, R. Gref, C. Boman, et al., Effects of raw material particle size distribution on the characteristics of Scots pine sawdust fuel pellets, Fuel Process. Technol. 89 (2008) 1324–1329, https://doi.org/10.1016/j.fuproc.2008.06.001.

[21] W. Stelte, J.K. Holm, A.R. Sanadi, S. Barsberg, J. Ahrenfeldt, U.B. Henriksen, Fuel pellets from biomass: the importance of the pelletizing pressure and its dependency on the processing conditions, Fuel 90 (2011) 3285–3290, https://doi.org/10.1016/j.fuel.2011.05.011.

[22] J. Xu, R. Widyorini, H. Yamauchi, S. Kawai, Development of binderless fiberboard from kenaf core, J. Wood Sci. 52 (2006) 236–243, https://doi.org/10.1007/s10086-005-0770-3.

[23] P. Lehtikangas, Quality properties of pelletised sawdust, logging residues and bark, Biomass Bioenergy 20 (2001) 351–360, https://doi.org/10.1016/S0961-9534(00)00092-1.

[24] W. Stelte, J.K. Holm, A.R. Sanadi, S. Barsberg, J. Ahrenfeldt, U.B. Henriksen, A study of bonding and failure mechanisms in fuel pellets from different biomass resources, Biomass Bioenergy 35 (2011) 910–918, https://doi.org/10.1016/j.biombioe.2010.11.003.

[25] N. Guigo, A. Mija, L. Vincent, N. Sbirrazzuoli, Molecular mobility and relaxation process of isolated lignin studied by multifrequency calorimetric experiments, Phys. Chem. Chem. Phys. 11 (2009) 1227–1236, https://doi.org/10.1039/B812512K.

[26] J. Bouajila, P. Dole, C. Joly, A. Limare, Some laws of a lignin plasticization, J. Appl. Polym. Sci. 102 (2006) 1445–1451, https://doi.org/10.1002/app.24299.

[27] L. Riva, H.K. Nielsen, Ø. Skreiberg, L. Wang, P. Bartocci, M. Barbanera, et al., Analysis of optimal temperature, pressure and binder quantity for the production of biocarbon pellet to be used as a substitute for coke, Appl. Energy 256 (2019) 113933, https://doi.org/10.1016/j.apenergy.2019.113933.

[28] R.I. Ismail, C.Y. Khor, A.R. Mohamed, Pelletization temperature and pressure effects on the mechanical properties of khaya senegalensis biomass energy pellets, Sustainability 15 (2023) 7501, https://doi.org/10.3390/su15097501.

[29] T.R. Sarker, V.B. Borugadda, V. Meda, A.K. Dalai, Optimization of pelletization process conditions and binder concentration for production of fuel pellets from oat hull and quality evaluation, Biomass Bioenergy 174 (2023) 106825, https://doi.org/10.1016/j.biombioe.2023.106825.

[30] N.P.K. Nielsen, D.J. Gardner, T. Poulsen, C. Felby, Importance of temperature, moisture content, and species for the conversion process of wood residues into fuel pellets, Wood Fiber Sci. (2009) 414–425.

[31] M. Kovacova, M. Matúš, P. Križan, J. Beniak, Design theory for the pressing chamber in the solid biofuel production process, Acta Polytech. 54 (2014) 28–34, https://doi.org/10.14311/AP.2014.54.0028.

[32] R. Čolović, Đ. Vukmirović, R. Matulaitis, S. Bliznikas, V. Uchockis, V. Juškienė, et al., Effect Of Die Channel Press Way Length on Physical Quality of Pelleted Cattle Feed, 2010.

[33] N. Mišljenović, R. Čolović, Đ. Vukmirović, T. Brlek, C.S. Bringas, The effects of sugar beet molasses on wheat straw pelleting and pellet quality. A comparative study of pelleting by using a single pellet press and a pilot-scale pellet press, Fuel Process. Technol. 144 (2016) 220–229, https://doi.org/10.1016/j.fuproc.2016.01.001.

[34] J. Hu, T. Lei, S. Shen, Q. Zhang, Specific energy consumption regression and process parameters optimization in wet-briquetting of rice straw at normal temperature, BioResources 8 (2012) 663–675, https://doi.org/10.15376/biores.8.1.663-675.

[35] S.K. Nielsen, M. Mandø, A.B. Rosenørn, 1D Model for Investigation of Energy Consumption and Wear in Die Designs Used for Biomass Pelleting. European Biomass Conference and Exhibition Proceedings 2018;26th EUBCE-Copenhagen, 2018, pp. 550–558, https://doi.org/10.5071/26thEUBCE2018-2CO.13.1.

[36] S.K. Nielsen, M. Mandø, Experimental and numerical investigation of die designs in biomass pelleting and the effect on layer formation in pellets, Biosyst. Eng. 198 (2020) 185–197, https://doi.org/10.1016/j.biosystemseng.2020.08.010.

[37] A. Sadeq, D. Heinrich, S. Pietsch-Braune, S. Heinrich, Influence of oscillating water content on the structure of biomass pellets, Powder Technol. 426 (2023) 118631, https://doi.org/10.1016/j.powtec.2023.118631.

[38] A. Sadeq, A. Frank, M. Tyslik, J. Jägers, S. Pietsch-Braune, V. Scherer, et al., Influence of cyclic water content changes during long-term storage on the mechanical stability of wood pellets, Powder Technol. 428 (2023) 118866, https://doi.org/10.1016/j.powtec.2023.118866.

[39] C. Tenorio-Monge, R. Moya-Roque, J. VALAERT, Characterisation of pellets made from oil palm residues in Costa Rica, JOPR 28 (2016) 198–210, https://doi.org/10.21894/jopr.2016.2802.08.

[40] T. Wongsiriamnuay, N. Tippayawong, Effect of densification parameters on the properties of maize residue pellets, Biosyst. Eng. 139 (2015) 111–120, https://doi.org/10.1016/j.biosystemseng.2015.08.009.

[41] A. Tilay, R. Azargohar, M. Drisdelle, A. Dalai, J. Kozinski, Canola meal moisture-resistant fuel pellets: Study on the effects of process variables and additives on the pellet quality and compression characteristics, Ind. Crop. Prod. 63 (2015) 337–348, https://doi.org/10.1016/j.indcrop.2014.10.008.

[42] Compression and Springback Properties of Hardwood and Softwood Pellets:: BioResources n.d. https://bioresources.cnr.ncsu.edu/ (accessed May 24, 2024).

[43] A.A. Siyal, Y. Liu, X. Mao, B. Ali, S. Husaain, J. Dai, et al., Characterization and quality analysis of wood pellets: effect of pelletization and torrefaction process variables on quality of pellets, Biomass Convers. Biorefinery 11 (2021) 2201–2217, https://doi.org/10.1007/s13399-020-01235-6.

[44] M.J. O'Dogherty, J.A. Wheeler, Compression of straw to high densities in closed cylindrical dies, J. Agric. Eng. Res. 29 (1984) 61–72, https://doi.org/10.1016/0021-8634(84)90061-1.

[45] K. Theerarattananoon, F. Xu, J. Wilson, R. Ballard, L. Mckinney, S. Staggenborg, et al., Physical properties of pellets made from sorghum stalk, corn Stover, wheat straw, and big bluestem, Ind. Crop. Prod. 33 (2011) 325–332, https://doi.org/10.1016/j.indcrop.2010.11.014.

[46] P. Sui Lam, Z. Tooyserkani, L. Jafari Naimi, S. Sokhansanj, Pretreatment and Pelletization of Woody Biomass, in: Z. Fang (Ed.), Pretreatment Techniques for Biofuels and Biorefineries, Springer, Berlin, Heidelberg, 2013, pp. 93–116, https://doi.org/10.1007/978-3-642-32735-3_5.

[47] M. Kashaninejad, L.G. Tabil, Effect of microwave–chemical pre-treatment on compression characteristics of biomass grinds, Biosyst. Eng. 108 (2011) 36–45, https://doi.org/10.1016/j.biosystemseng.2010.10.008.

[48] M. Thomas, T. van Vliet, A.F.B. van der Poel, Physical quality of pelleted animal feed 3. Contribution of feedstuff components, Anim. Feed Sci. Technol. 70 (1998) 59–78, https://doi.org/10.1016/S0377-8401(97)00072-2.

[49] I.N. Manickam, D.D. Ravindran, D.P. Subramanian, Biomass densification methods and mechanism, Cogener. Distrib. Gener. J. (2006), https://doi.org/10.1080/15453660609509098.

[50] L. Bennamoun, N.Y. Harun, M.T. Afzal, Effect of storage conditions on moisture sorption of mixed biomass pellets, Arab. J. Sci. Eng. 43 (2018) 1195–1203, https://doi.org/10.1007/s13369-017-2808-4.

[51] C. Karunanithy, K. Muthukumarappan, A. Donepudi, Moisture sorption characteristics of switchgrass and prairie cord grass, Fuel 103 (2013) 171–178, https://doi.org/10.1016/j.fuel.2012.05.004.
[52] B. Krupińska, I. Strømmen, Z. Pakowski, T.M. Eikevik, Modeling of sorption isotherms of various kinds of wood at different temperature conditions, Dry. Technol. 25 (2007) 1463–1470, https://doi.org/10.1080/07373930701537062.
[53] M. Fredriksson, P. Johansson, A method for determination of absorption isotherms at high relative humidity levels: measurements on lime-silica brick and Norway spruce (Picea abies (L.) Karst.), Dry. Technol. 34 (2016) 132–141, https://doi.org/10.1080/07373937.2015.1041035.
[54] J.-G. Salin, Drying of liquid water in wood as influenced by the capillary fiber network, Dry. Technol. 26 (2008) 560–567, https://doi.org/10.1080/07373930801944747.
[55] T. Deng, A.M. Alzahrani, M.S. Bradley, Influences of environmental humidity on physical properties and attrition of wood pellets, Fuel Process. Technol. 185 (2019) 126–138, https://doi.org/10.1016/j.fuproc.2018.12.010.
[56] S. Graham, C. Eastwick, C. Snape, W. Quick, Mechanical degradation of biomass wood pellets during long term stockpile storage, Fuel Process. Technol. 160 (2017) 143–151, https://doi.org/10.1016/j.fuproc.2017.02.017.
[57] L. Cutz, U. Tiringer, H. Gilvari, D. Schott, A. Mol, W. de Jong, Microstructural degradation during the storage of biomass pellets, Commun. Mater. 2 (2021) 1–12, https://doi.org/10.1038/s43246-020-00113-y.
[58] I.D. Hartley, L.J. Wood, Hygroscopic properties of densified softwood pellets, Biomass Bioenergy 32 (2008) 90–93, https://doi.org/10.1016/j.biombioe.2007.06.009.
[59] J.S. Lee, S. Sokhansanj, A.K. Lau, C.J. Lim, Physical properties of wood pellets exposed to liquid water, Biomass Bioenergy 142 (2020) 105748, https://doi.org/10.1016/j.biombioe.2020.105748.
[60] J.S. Lee, S. Sokhansanj, A.K. Lau, J. Lim, X.T. Bi, Moisture adsorption rate and durability of commercial softwood pellets in a humid environment, Biosyst. Eng. 203 (2021) 1–8, https://doi.org/10.1016/j.biosystemseng.2020.12.011.
[61] C. El Hachem, K. Abahri, R. Bennacer, Microscopic swelling analysis of spruce wood in sorption cycle, Energy Procedia 139 (2017) 322–327, https://doi.org/10.1016/j.egypro.2017.11.215.
[62] D. Kosiachevskyi, C. El Hachem, K. Abahri, R. Bennacer, M. Chaouche, Biomaterials heterogeneous displacement, strain and swelling under hydric sorption/desorption: 2D image correlation on spruce wood, Constr. Build. Mater. 286 (2021) 122997, https://doi.org/10.1016/j.conbuildmat.2021.122997.
[63] E.T. Engelund, L.G. Thygesen, S. Svensson, C.A.S. Hill, A critical discussion of the physics of wood–water interactions, Wood Sci. Technol. 47 (2013) 141–161, https://doi.org/10.1007/s00226-012-0514-7.
[64] S. Graham, I. Ogunfayo, M.R. Hall, C. Snape, W. Quick, S. Weatherstone, et al., Changes in mechanical properties of wood pellets during artificial degradation in a laboratory environment, Fuel Process. Technol. 148 (2016) 395–402, https://doi.org/10.1016/j.fuproc.2016.03.020.
[65] O. Williams, S. Taylor, E. Lester, S. Kingman, D. Giddings, C. Eastwick, Applicability of mechanical tests for biomass pellet characterisation for bioenergy applications, Materials 11 (2018) 1329, https://doi.org/10.3390/ma11081329.
[66] H. Gilvari, W. de Jong, D.L. Schott, Breakage behavior of biomass pellets: an experimental and numerical study, Comput. Part. Mech. 8 (2021) 1047–1060, https://doi.org/10.1007/s40571-020-00352-3.
[67] DIN 863-1:2017-02, Geometrische Produktspezifikation_(GPS)_- Messschrauben_-Teil_1: Bügelmessschrauben; Grenzwerte für Messabweichungen n.d. doi:10.31030/2603372.
[68] E. Andò, Experimental Investigation of Microstructural Changes in Deforming Granular Media Using x-Ray Tomography, 2013.